We thank the reviewers for their constructive criticism on our manuscript. We have responded to all comments made by the reviewers as the text below shows. The answers are structured as follows: (1) comment of the referee in **black**, (2) answer in **red** and (3) rewritten text parts in **blue**.

Anonymous Referee #1 / Received and published: 24 October 2015

Specific Comments

1. The major issue I have is that the authors assume an IG TTD, and attributes differences between model and data to sub or super saturation of the tracers (or SF6 remaining from deliberate tracer release. However, another reason (that I think is more likely)is that the TTD is not well described by a single IG TTD. The authors need to explore this possibility. In the Stoven et al. (2015) they did some calculations using two-IG TTDs, and I think similar calculations need to be done here. Is it possible to reproduce the SF6 and CFC12 using a two-IG TTD, and if so how different is the calculated Cant?

Our assumption on saturation effects opens up new perspectives on possible error sources when using ocean ventilation models at high latitudes. So we do not know yet if saturation effects or complex mixing processes are responsible for the specific concentration ratios of transient tracers in these ocean areas. The problem is that the system of equation of the 2IG-TTD is undetermined due to the five free parameters (two "Deltas", two "Gammas" and the ratio between the two water-mass abundances alpha) combined with only two transient tracers. Nevertheless we did some calculations using the 2IG-TTD which are shown in the figure below. Here we used the same assumptions as in Stöven et al. (2014) since it incorporates one very advective (Delta/Gamma=0.6) and one more diffusive water parcel (Delta/Gamma=1.4). It can be seen that most of the data points are still outside the application range unaffected by the alpha-parameter.

Section 2.3

"Another approach is based on a linear combination of two IG-TTDs which can be used to describe more complex ventilation pattern (Eq. 3) (Waugh et al., 2002). The variables of this model are $\Delta_{1,2}$ and $\Gamma_{1,2}$ of the two IG-TTDs and α which describes the ratio between both distributions. The main problem of applying this method is, that five free parameters need to be determined. Hence, this model combination can be constrained with five transient tracers with sufficiently different input functions. Alternatively, predefined parameters can be used (Stöven and Tanhua, 2014)."

Section 3.3

"Another approach is provided by the linear combination of two IG-TTDs. Since we only have the data of two transient tracers, we used the same predefined parameters as described in Stöven and Tanhua (2014) which includes one more diffusive water parcel (Δ_1/Γ_1 = 1.4) and one very advective water parcel (Δ_2/Γ_2 = 0.6). Figure 6 shows, similar to Fig. 5, the validity area of the linear combination of two IG-TTDs for different α of 0.2, 0.5 and 0.8. Although this combination describes several scenarios from highly advective to diffusive mixing of two distributions, it can be seen that most of the observed data points are still outside the validity area. Thus, the tracer age

relationship between CFC-12 and SF_6 can neither be described by the IG-TTD nor a linear combination of two IG-TTDs."

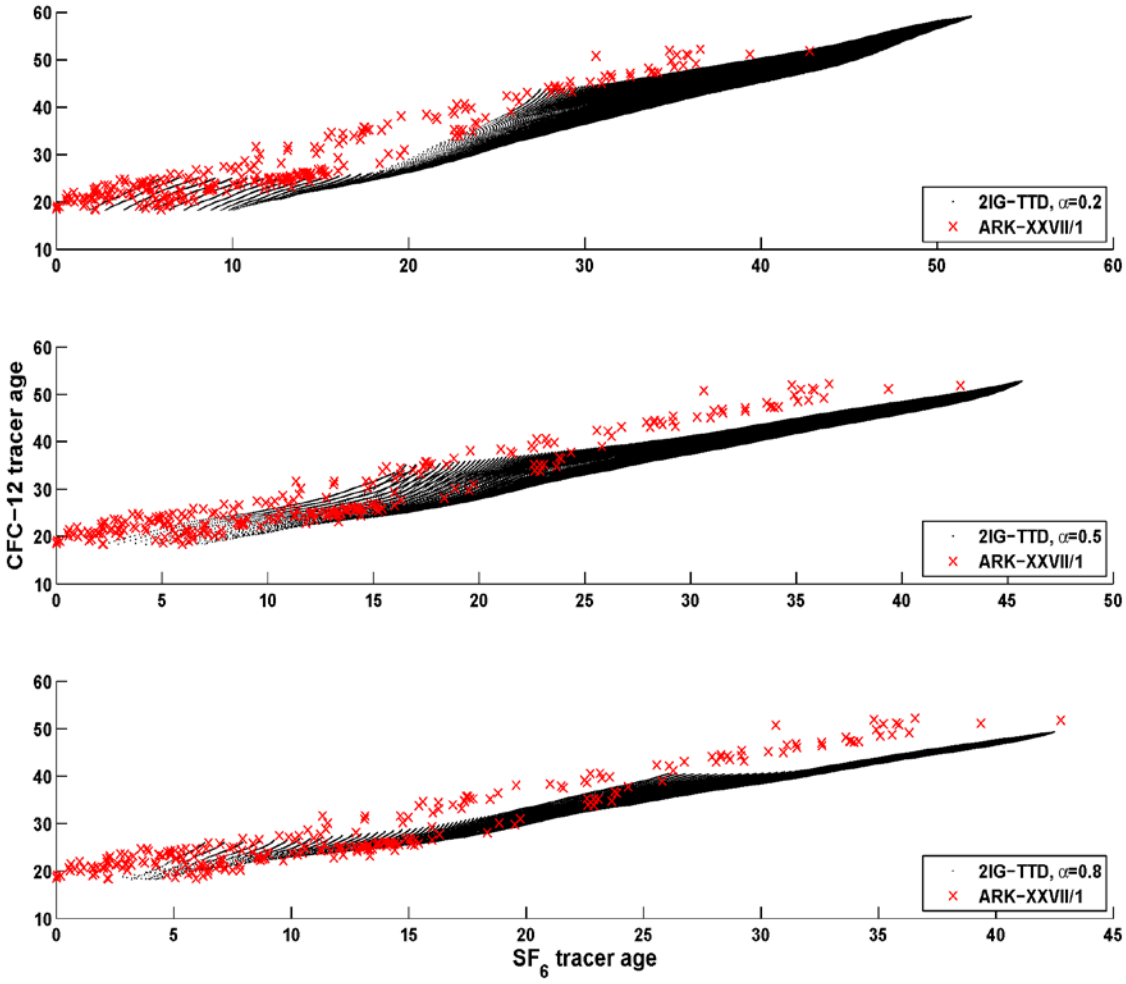

2. The discussion in first few sentencing of section 2.3 uses "transit time distribution", "Green's function" and "age spectra" somewhat interchangeably, which is confusing. I think they mean the same thing for all 3 terms and should just use one. If they mean different things by each term then they need to describe this better.

Text part rewritten.

Section 2.3

"A transit time distribution (TTD) model (Eq. 1) describes the propagation of a boundary condition into the interior of the ocean and is based on the Green's function (Hall and Plumb,1994). Here, c(ts;r) is the specific tracer concentration at year ts and location r, c0(ts -t) the boundary condition described by the tracer concentration at source year ts-t and G(t) the transit time distribution of the tracer. The exponential

term corrects for the decay rate of radioactive transient tracers. Equation 2 provides a possible solution of the TTD model, based on a steady and one-dimensional advective velocity and diffusion gradient (Waugh et al., 2003). It is known as the Inverse-Gaussian transit time distribution (IG-TTD) where G(t) is defined by the width of the distribution (Δ), the mean age (Γ) and the time range (t)…"

3. There is no discussion of application of SF6 as age tracer. Although CFC12 can't be used in "young" waters, SF6 can.

Additional text added.

Section 2.3
"Note that the use of CFC-12 as transient tracer is limited to concentrations below the recent atmospheric level since the production of CFC-12 was phased out in the early 1990s so that the depletion rate exceeds the emission rate since the early 2000s. This causes indistinct time information of CFC-12 since one concentration describes two dates in the atmospheric history. To this end, the use of CFC-12 is restricted to water masses with concentrations below the current atmospheric concentration limit. The emission rate of SF6 still exceeds the depletion rate so that the atmospheric concentration is still increasing. SF6 thus provides distinct age information of water masses over the complete concentration range."

4. On page 2203 evidence is presented that suggests that the "excess SF6" is not due to deliberate tracer release, but on pg 2208 (line 29) this is given as one of the reasons. I am confused, do the authors think this is a likely cause? If not then should not be in the conclusions.

We think that both sources of excess SF_6 play a role in the Nordic Seas and Arctic Ocean. The ratio between natural and anthropogenic supersaturation cannot be determined by the data at hand. However, compared to the observations in the Southern Ocean, we think that natural supersaturation by bubble effects can have larger impacts than previously thought. The text might have been misleading in this case and was rewritten to clarify this crucial point.

Section 3.4
"One possibility refers to the deliberate tracer release experiment in 1996 where 320kg (~2190mol) of SF6 were introduced into the central Greenland Sea (Watson et al., 1999). (…) However, CFC-12 and SF6 data of the Southern Ocean (Stöven et al., 2015) shows similar tracer age relationships compared to the Fram Strait data but with no influence of deliberately released SF6. This indicates that another source of excess SF6 may exist which is much larger than the source of the tracer release experiment."

Section 4
"We assumed that the different tracer age relationships are due to different saturation effects on the tracers during water mass formation and still existing offsets of the SF6 concentrations caused by the deliberate tracer release experiment in the Greenland Sea in 1996."

5. Should the Stöven et al. (2014) references on pg 2203 be the 2015 paper?

Yes indeed. Reference corrected.

6. "is supposed to be" indicates that the authors don't think this is the reason. If they authors think the applicability is limited because of these factors then remove "supposed to be".

Yes, we do not think that complex ventilation pattern are limiting the application of the model. However, ventilation models are always based on restrictive assumptions and only provide a simplified view on natural processes. The question is, if the model is too far away from reality or if other circumstances such as saturation effects lead to wrong assumptions. Here again, the text was rewritten for a better understanding.

Section 3.8

"We showed that neither the IG-TTD nor linear combinations of the model can describe the tracer age relationships between CFC-12 and SF6 in the Fram Strait. This means that either the models are not suitable to describe the prevailing ventilation pattern or that there are other reasons which lead to the specific concentration ratios. Here we focused on the second case which incorporates the assumptions that the tracer age relationships are related to different saturation states of the transient tracers and, furthermore, that the simple IG-TTD model can describe the ventilation processes of all water masses in the Fram Strait. The uncertainties of our approach thus correspond to the chosen shape of the IG-TTD, i.e. the unity ratio of Δ/Γ = 1.0, and the uncertainties of the measurement precision of the transient tracers and apparent transient tracers (see section 3.6 above). Further uncertainties are related to processes which influence the gas exchange and thus the boundary conditions of the tracers. This includes the important but yet rarely investigated impact of sea ice cover, sea ice formation and sea ice melting processes as well as bubble effects during heavy wind conditions."

We thank the reviewers for their constructive criticism on our manuscript. We have responded to all comments made by the reviewers as the text below shows. The answers are structured as follows: (1) comment of the referee in **black**, (2) answer in **red** and (3) rewritten text parts in **blue**.

Anonymous Referee #2
Received and published: 28 October 2015

In the reviewed paper authors propose several hypotheses, assumptions, simplifications and finally - conclusions.
Generally, the paper deals with three distinct issues: 1) direct observation of transient tracers (CFC-12 and SF6) distribution in summer 2012; 2) use of IG-TTD method for comparison of theoretically calculated and observed tracers ages and for anthropogenic carbon calculation based only on CFC-12; 3) transport of DIC and previously calculated anthropogenic offset in the upper/intermediate layer across the Fram Strait.
While the first part is rather trivial, the second is the most developed/discussed, the third is controversial and only briefly analyzed in the manuscript. Nevertheless, presentation of any new observations concerning the ocean uptake capability for anthropogenic gases is valuable for the scientific community, especially considering the fact that the ice-covered polar regions are still under-sampled. The theories introduced in the manuscript, even though arguable, are interesting. Thus, in my opinion, the submitted paper should be published after some corrections and additional explanations – this means a major revisions.

Below are some specific comments which may help re-think the presented material:

Title
The title is misleading – it suggests broader look, as well as longer time perspective.

Title changed to "Transient tracer distribution in the Fram Strait in 2012 and inferred anthropogenic carbon content and transports"

Abstract
Page 2190 - Current velocity measurements along the same section - it should be mentioned the measurements were performed in the previous years – mean flow.

We now make it clear in that sentence that the mean velocities from 2002 to 2010 are used.

"Mean current velocity measurements along the same section from 2002-2010 were used to estimate the net flux of DIC and anthropogenic carbon by the boundary currents through the Fram Strait above 840m."

Introduction
Page 2191 - The elevated heat flux of warm Atlantic Water into the Arctic Ocean – where and when? Higher temperature or volume of AW?

Text added.

"The temperature of the Atlantic Water flowing into the Arctic Ocean in the Fram Strait has warmed since 1997 (Beszczynska-Möller et al., 2012), which increased the heat flux into the Arctic."

Page 2192 - a short meridional section along the fast ice edge in 2012 – how valuable is this section for the overall analysis and discussion? The data from several (1-2?) stations appear only in Figure 2.

This section shows no differences in the horizontal distribution so that the zonal range of the fast ice section is already described by the corresponding longitude range of the zonal section. This particular section is not used for the analysis but nevertheless we introduce the full data set at this point. Additional text added.

Section 2.1

"The meridional section along the fast ice edge was only sampled for CFC-12 and SF_6 which shows no differences in the horizontal tracer distributions compared to the corresponding longitude range of the zonal section. Therefore we have only used the zonal section for the following analysis."

Data and Methods

Water transport data

Page 2194 - gross assumption applied by authors is that the mean velocity field calculated for the years 2002-2010 represents particular situation in summer 2012. This is based on the authors' statement of small interannual changes and no trend in the flow. Previous studies indicated a non-steady situation, which is also confirmed by a recent work (Hansen et al., 2015). This study is based on a combination of the in-situ data (moorings and CTD stations) and satellite altimetry, and it shows a distinct trend in volume, heat and salt transports in the AW layer across the Faroe Shetland Channel (FSC) – the main AW entrance into the Nordic Seas. The mentioned paper also points out high interannual and seasonal variabilities. Since the AW transport across the FSC has increased in the recent period (9_8% in the last 2 decades), transport through the Fram Strait/BSO is also most likely to increase. Even though it is not clear how this additional volume has been distributed (FS, BSO and recirculation in the Norwegian and Greenland Seas), it is rather hard to claim that there is no trend in fluxes in the Fram Strait at all.

We thank the reviewer for his/her points here, but we disagree with the conclusions. While there may have been a trend at the Faroe Bank Channel (at the other side of the Nordic Seas), no statistically significant interannual trends in the volume transport through the Fram Strait between 1997 and 2010 were observed (Beszczynska-Möller et al, 2012). These observations are based on the extensive mooring data set in the Fram Strait and in our opinion they are hence more insightful about what is happening in Fram Strait than the observations in the Faroe Bank Channel and the speculations about how those changes may or may not be then divided up between the Barents Sea inflow, the Fram Strait inflow and the recirculations in the Fram Strait

and the Nordic Seas. There has, however, been a significant change in the temperature of the inflowing Atlantic Water in the Fram Strait.
One aim of our manuscript was to estimate transports of anthropogenic carbon through the Fram Strait. Transports are the product of concentrations times velocities integrated over an area. The assumptions which we make (and which in our opinion is not "gross") is that the trace gas concentrations change relatively slowly between years with no significant seasonal changes. Hence, we can take the concentrations from summer 2012 to be informative about other seasons and years within some range from 2012. On the other hand, we know that velocities change strongly between seasons, but not significantly between years. It follows that the measured (2002-2010) long term average volume transport is representative of the volume transport through Fram Strait in the late 2000s / early 2010s. Likewise, the measured Cant concentrations in summer 2012 are representative for the Cant concentrations in the late 2000s / early 2010s. The product of the two is then our estimate of the Cant transport through the Fram Strait in the late 2000s / early 2010s.

Section 2.4
"We then proceed to estimate transports of anthropogenic carbon through Fram Strait. Transports are the product of concentrations times velocities integrated over an area. We assume that the trace gas concentrations change relatively slowly between years and that there are no significant seasonal changes. Hence, we can take the concentrations from summer 2012 to be informative about other seasons and years within some range from 2012. On the other hand, it is known that velocities change strongly between seasons (and on shorter time scales), but on average not significantly between years in the Fram Strait (Beszczynska-Möller et al, 2012). It follows that the measured (2002-2010) long term average volume transport is representative of the volume transport through Fram Strait in the late 2000s/early 2010s. Likewise, the measured Cant concentrations in summer 2012 are representative for the Cant concentrations in the late 2000s/early 2010s. The product of the two is then our estimate of the Cant transport through the Fram Strait in the late 2000s/early 2010s."

The second assumption states that the net transport beneath the upper/intermediate layer (the depth of the FBC sill being a part of the Greenland-Scotland-Ridge is 840 not 750 m) is equal to zero. Previous studies take into consideration various net values in the deep flow in the Fram Strait - from net southward transport (Schlichtholz and Houssais, 1999; Beszczynska-Möller et al., 2012, Marnela et al., 2013) to balanced exchange (Tsubouchi et al., 2012; Von Appen et al., 2015). The authors also point out that the moored instruments at the 78°50'N section do not resolve the mesoscale features and the local bathymetry very well.

We agree with these points raised by the reviewer, but both tracers show a homogenous zonal distribution below 1500 m so that any net flux would not change the inventory of anthropogenic carbon below this depth. Net fluxes in the depth range between 840 m and 1500 m might indeed contribute to either the Arctic or the Nordic Seas reservoir but this is still an enclosed basin-basin interaction.

Section 2.2
"The estimate of the volume transport across the Fram Strait below 840m from the moorings is more complicated. The method of Beszczynska-Möller et al. (2012) which was developed to study the fluxes in the West Spitsbergen Current predicts a

net southward transport of 3,2Sv below 840m. This is unrealistic given that there are no connections between the Nordic Seas and the Arctic Ocean below the sill depth of the Greenland-Scotland Ridge (840m) other than the Fram Strait. No vertical displacements of isopycnals in these two basins are observed that would suggest a non-zero net transport across the Fram Strait below 840m (von Appen et al.,2015a). The large net transport inferred by Beszczynska- Möller et al. (2012) is due to the insufficient horizontal resolution of the mooring array to explecitly resolve the westward flow of the recirculation and the mesoscale eddies. For these reasons we assume a net flux of 0Sv across the Fram Strait for the deep waters below 840m."

Another explanation of the variable southward deep flow through the Fram Strait is discussed in connection to extreme air-sea exchange in the Barents Sea in strong winters (Moat et al., 2014). This study underlines the importance of the variable surface conditions in only one of many marginal seas affecting the deep circulation in the Fram Strait.

Moat et al (2014) discuss velocity anomalies in Fram Strait of less than 0.5cm/s as a result of processes in the Barents Sea. Those are tiny numbers compared to the total flows through the Fram Strait (both in the upper and lower water columns). Therefore, the differences between years resulting from the processes discussed there are small compared to the long-term average volume transports. Furthermore, it is not clear how those processes should be integrated into our analysis where the snapshot of measured Cant has to be interpreted on a larger time horizon to be insightful.

TTD method

Page 2195 – The D/G ratio equal to 1 seems to be used in many water mass productive regions, but is it best for the Fram Strait (strong advection)? In fact, the Section 3.3 answers this question.

It can be expected that the boundary currents passing the Fram Strait show higher mean velocities and are probably better described by a higher advective share (i.e a lower Delta/Gamma ratio) at this particular point. However, this only accounts for the narrow Fram Strait. In contrast, the TTD model describes constant mixing processes affecting the water mass from its source, i.e. where the water parcel lost contact with the atmosphere, to the point of measurement which is the Fram Strait section in our case. The water mass characteristics are not based on the particular measurement region but are rather constantly affected along the flow pathway, e.g. in the Nordic Seas or Arctic Ocean. It can be discussed if the assumption on constant mixing parameters (IG-TTD) should be replaced by a more variable / dynamic model with changing mixing conditions along the flow pathway. To our knowledge there are no such models available.

Section 3.3

"Based on the raw field data, and on assumptions implemented in the IG-TTD (like constant mixing processes along the flow pathway as well as constant saturation of the gases at the surface before entering deeper layers), the IG-TTD or linear combinations of the IG-TTD can only partly describe the ventilation pattern of water masses in the Fram Strait."

Page 2195 - similarly as for the CFCs input functions - it was recently described (Fang et al., 2014) that around the year 2000 there was a reversal in the global SF6 emission trend, from decreasing to increasing, which was probably caused by increasing emissions in the East Asian countries. This additional amount shall be detectable in the AO surface water through the Pacific inflow.

The atmospheric SF_6 concentration in the northern/southern hemisphere as well as the global mean is still increasing and never showed a decreasing trend such as it can be observed for the CFCs. See https://agage.mit.edu/ for more information. The reason for this is the long atmospheric life-time of SF_6 and the dispersive nature of the release to the atmosphere that tend to dampen annual variations in emission. The ocean tracer application of SF_6 is only dependent on the atmospheric concentration, which is well known.

Furthermore, the changing sea ice cover of the Arctic Ocean needs to be mentioned as a potential source of anthropogenic gases content in the Polar Water of the Pacific origin – a recent study (Ballinger and Sheridan, 2015) describes changes in the western Arctic freeze-up pattern suggesting the changing ocean–atmosphere heat exchanges connected with prolonged melt period as a cause. This is also most likely to apply to the Siberian shelf seas.

The gas-exchange in the Arctic Ocean is a very complex system since it involves melting and freezing processes, different types of ice cover, ice thickness etc. which is rarely described in the literature. Note that we provide an example of the model output of Shao et el. 2013 which show the extreme variability of tracer surface saturations in the Arctic Ocean in different regions. This model includes assumptions on ice cover but the real conditions probably highly deviate from the model output as we have shown for observed data in the Southern Ocean. There is a great potential for future investigations but there are no corresponding constraints available which can be used for our analysis. It is also not clear to what extent CO_2 and CFCs can equilibrate through ice cover; it is likely that the dis-equilibrium of CO_2 is larger than for CFCs due to the longer equilibrium time. This is certainly a source of uncertainty.

Section 3.6

"Furthermore it is unclear to what extent the time period and type of sea ice coverage as well as the sea ice formation and melting processes bias the pCO_2 and tracer saturations at high latitudes."

Results and discussion

Water masses in Fram Strait

Page 2197 – "Note that this water mass classification is not based on an optimum multi parameter analysis and only serves as an indication for this specific purpose" – what is the reason for this explanation? Would OMP analysis provide more accurate classification? If yes, why not using it with so many data collected? This would be an additional work but perhaps a little more certainty would be beneficial for this paper. If not, consider this sentence redundant.

For our purpose the clear definitions of water masses are sufficient to show the specific tracer characteristics of the different water masses. An OMP would provide the water type mixing ratios of different source regions which would be indeed interesting but these information would not improve the results of our analysis. Sentence removed.

Page 2197 – "the warm Polar Surface Water, defined by a potential temperature (Θ) >0, which comprises sea ice melt water due to interaction with warm Atlantic Water" – and due to solar radiation because it is summer.

Text added.

Section 3.1
"…,which comprises sea ice melt water due to interaction with warm Atlantic Water and due to solar radiation;…"

Page 2197 – "Return Atlantic Water which derives from sinking Atlantic Water due to cooling in the Arctic Ocean" – in the applied classification (Rudels, 2005) the RAWoriginates in the West Spitsbergen Current – it is the water that recirculates in the northern Greenland Sea, not the water making a long loop in the Arctic Ocean and coming back – this one is called the Arctic Atlantic Water (AAW). This is also inconsistent in Section 2.2 (Page 2194).

There is some inconsistency about the abbreviation of the Arctic Atlantic Water (AAW) which is also called the Return Atlantic Water (RAAW) but should not be mixed up with the expression of Recirculating Atlantic Water (RAW). We removed the expression "Return Atlantic Water – RAAW" from the manuscript and stick to Arctic Atlantic Water for this water mass.

Page 2197 – "the deep water masses are upper Polar Deep Water (uPDW), Canadian Basin Deep Water (CBDW) and Eurasian Basin Deep Water (EBDW) and the Nordic Seas Deep Water" – does the classification from 2005 still applies to these water masses? Are they within the range? The _S diagram would be helpful.

Von Appen et al (2015, Deep Sea Research) presents a TS diagram of Eurasian Basin Deep Water (EBDW) and Greenland Sea Deep Water (GSDW) and it shows that both water masses have warmed over the past two decades. By using a constant water mass definition (where the temperatures are not allowed to change over time), Langehaug and Falck (2012, Progress in Oceanography) incorrectly concluded that GSDW had disappeared from the deep Fram Strait. Hence, we do not distinguish between GSDW and EBDW here, but rather use a broader definition for those deep water masses. Such an analysis has not been done for the other deep water masses and we think that the current manuscript would not be the appropriate location to do so.

Transient tracer and DIC distributions

Page 2199 – "Both tracer maxima probably correspond to extensive ventilation events" – when and where? Obviously, this is more like guessing but indicate how little we still know about regions/periods favorable for the Greenland Sea convection.

We do not know where, when and how exactly this ventilation event occurred but we can see the signal in the tracer data. Text rewritten.

Section 3.2

"Both tracer maxima probably correspond to recently ventilated water which mainly affected the Arctic Intermediate Water and partly the Atlantic Water in the transition zone of both water masses. The Arctic Intermediate Water in the Fram Strait thus consists of recently ventilated areas and less ventilated areas which is also indicated by the large range of transient tracer concentrations."

Page 2199 – "0.2ppt of SF6" – is it not too close to the method accuracy?

This partial pressure of SF_6 is close to the detection limit of the used analytical system (0.1 fmol/kg) but not to the methods accuracy of ~ 0.06 fmol/kg.

Page 2200 – "two branches of tracer age relationships" – it is a misfortunate expression, since branches are associated with the water pathways. Perhaps "sets" would be better.

We now use "set" instead of branch for the tracer age structures.

Page 2200 – "show a transition to the upper branch" – perhaps it is better to say that two sets merge or have an intersection area.

Text rewritten.

Section 3.3

"Note that the Arctic Atlantic Water and upper Polar Deep Water merge with the upper set for a SF_6 tracer age larger than about 25 years."

Page 2200 – "However, the upper branch does not correspond to the unity ratio and, moreover, it is outside the validity area of the IG-TTD" – does this mean that only the results below 20 years from "the lower branch" can really be used in the validation process? Well, yes, the answer is on the next page.

The model is only valid for the minor part of the tracer data when applied as measured. We explain in detail that saturation effects are possible limiting factors of the IG-TTD and not complex ventilation pattern as usually suggested in other literature. A saturation correction of the tracer data can enable the application of the IG-TTD at high latitudes.

Section 3.3

"Nevertheless, by comparing the shape of the two field data sets with the shape of the black line in Fig. 5, it is noted that both sets show similar characteristics as the unity ratio or, generally, as IG-TTD based tracer age relationships. This opens up the possibility to use the IG-TTD the other way around,…"

Saturations and excess SF6

Page 2202 – “These new boundary conditions are then applied to the measured tracer concentrations and the IG-TTD” – it would be good to see these corrected data.

The offset does not change the distribution pattern. The figure below shows the saturation corrected CFC-12 section. If necessary we could include this figure into the manuscript but we don’t think that this is a must-have for the manuscript.

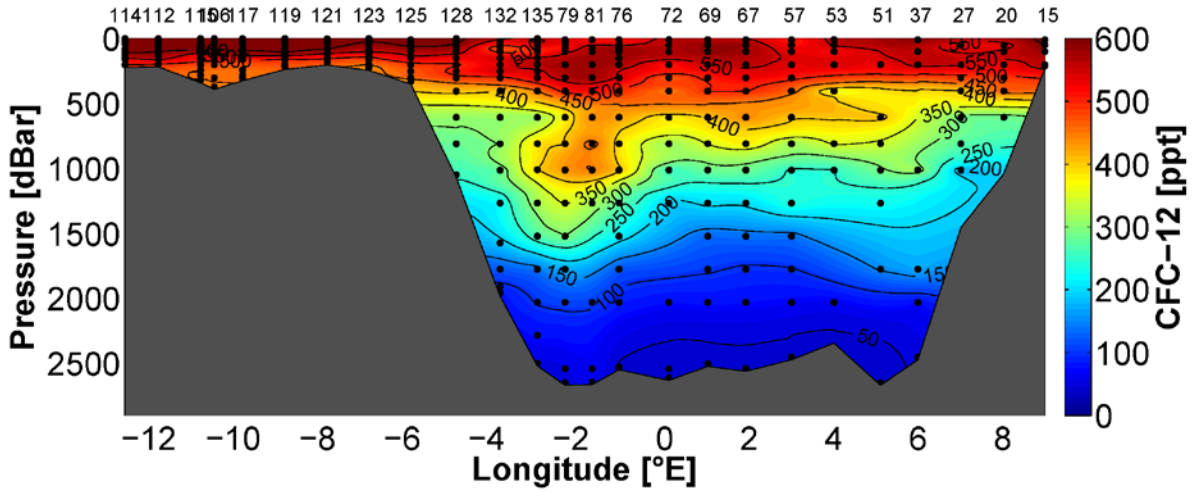

Page 2202 – “The SF6 excess is estimated using the corrected CFC-12 concentrations and the IG-TTD (Δ/Γ = 1.0)” – I still think that this ratio may be too low.

See explanation above

Page 2203 – “This indicates that probably an additional source of excess SF6 exists” – try to find an answer in references, it must be connected with the AW inflow.

We discuss the only two sources of excess SF_6 that we can think of; from the tracer release experiment and from supersaturation from bubbles injected to the water. We cannot think of any other source of SF_6.

Page 2203 – “the generally elevated tracer concentrations of CFC-12 and SF6 in the same area” – this contradicts with the conclusion from the Southern Ocean experiment on solubility.

No it does not. Both tracer distributions show generally elevated concentrations, i.e. indicate that this water parcel was recently ventilated by both tracers and not only by SF_6. The concentration ratio between both tracers can then be explained by bubble effects.

Generally, the theory of SF6 excess source for is interesting, yet perhaps more study

on gases solubility would be required. The previous paper (Alvarez and Gourcuff, 2010) indicates the difference between Cant and CFCs solubility affecting the gases concentration and transports. Could it be the case?

This is two different problems that the reviewer point out here: 1) difference in saturation between the transient tracers SF_6 and CFC12 that makes it more difficult to characterize the transit time distribution, and 2) the difference between the solubility of anthropogenic carbon and transient tracers. It is well known that the equilibrium process for CO_2 (i.e. anthropogenic carbon) is about 10 times slower than for CFCs which leads to issues in areas where the water mass in in contact with the atmosphere for a short time only, so that an uptake of transient tracers will be accompanied by a small uptake of anthropogenic carbon. We have focused our discussion here on point 1, the potential difference in solubility of SF_6 and CFC12 that are commonly assumed to be close to equal. This is thus a new aspect, and not directly related to the discussion in Alvarez and Gourcuff (2010).

Anthropogenic carbon and mean age

Page 2204 – "show the highest mean current velocities in Fram Strait (see Sect. 3.7 below)" – there is no information about the mean currents velocity in Section 3.7 and nowhere in the manuscript (only transports).

Thanks for pointing this out. We removed the reference from Section 3.7 and substituted it by a reference from Beszczynska-Möller et al (2012).

Sensitivities on anthropogenic carbon

Page 2207 – "The mean flux of deep water layers below 750m was taken to be 0Sv and therefore not considered for this estimate" – this assumption means that only the upper/intermediate transport is considered in that manuscript, not the whole FS.

This is true. We now mention this explicitly in the abstract and at the end of the introduction. The reason for this is two-fold: 1) we are not able to estimate a net transport based on the mooring data that we have, and 2) the zonal distribution of Cant is very similar at deeper depths so that a net north/south transport would not mean much in terms of Cant transport.

Section 3.7

"Furthermore, any net flux below 1500m would not change the anthropogenic carbon inventory of the Nordic Seas or the Arctic Ocean due to the homogeneous distribution of anthropogenic carbon at these depths. The depth range between 840m and 1500m might contribute to either the Arctic or the Nordic Seas reservoir but it is still an enclosed basin-basin interaction."

Page 2207 – "we cannot with great confidence decide whether more anthropogenic carbon is transported into or out of the Arctic region through the Fram Strait" – this is the weak point of the manuscript, though perhaps it could lead to some additional studies (better sampling coverage and current measurements).

We agree that it is disappointing that we are not able to provide a clear consensus of the net Cant transport. Although there are difficulties in accurately determine the Cant concentration (that we also discuss in the manuscript), the by far largest source of uncertainty is the transport estimates. This uncertainty in transport estimates is known by the operators of the current array and a new design of the array has been implemented to remedy this weakness. In that respect, the high uncertainty in transport reported here has contributed to the need of the re-design.

Uncertainties

Page 2207 – "is supposed to be limited by complex water mass mixing and ventilation patterns" – this contradicts the theory of small mixing impact on the differences in the tracers age relationships.

Text rewritten

Section 3.8
"We showed that neither the IG-TTD nor linear combinations of the model can describe the tracer age relationships between CFC-12 and SF6 in the Fram Strait. This means that either the models are not suitable to describe the prevailing ventilation pattern or that there are other reasons which lead to the specific concentration ratios. Here we focused on the second case which incorporates the assumptions that the tracer age relationships are related to different saturation states of the transient tracers and, furthermore, that the simple IG-TTD model can describe the ventilation processes of all water masses in the Fram Strait. The uncertainties of our approach thus correspond to the chosen shape of the IG-TTD, i.e. the unity ratio of Δ/Γ = 1.0, and the uncertainties of the measurement precision of the transient tracers and apparent transient tracers (see section 3.6 above). Further uncertainties are related to processes which influence the gas exchange and thus the boundary conditions of the tracers. This includes the important but yet rarely investigated impact of sea ice cover, sea ice formation and sea ice melting processes as well as bubble effects during heavy wind conditions."

Page 2207 – "the IG-TTD model is valid for all water masses in the Fram Strait" – it was showed that the model is valid for some water masses, not for all of them.

See answer above

Page 2208 – "recommend the use of data from the subsurface layer" – recommend using the data. Which data? Salinity?

As it is described in the foregoing sentence it is the salinity/alkalinity data from the subsurface layer and not from the surface. Sentence rewritten for a better understanding.

Section 3.8
"The determination of the preformed alkalinity highly depends on the used method. Here we used the linear relationship between surface alkalinity and salinity which is a commonly used method. However, other authors recommend the use of alkalinity /

salinity data from the subsurface layer (Vazquez-Rodriguez et al., 2012) or the surface temperature and salinity dependencies (Lee et al., 2006)."

Conclusions

This part is more of a summary than actual conclusions. There is no new information which has not been already mentioned in the previous sections.

We added a new text part which provides more information about the essence of the manuscript.

Section 4

"The theory of saturations effects on transient tracers requires more targeted experiments and data acquisition from high latitudes to get proven or rejected. However, this approach should not contradict the assumptions on complex ventilation pattern but should rather contribute to a better understanding and analysis of the dynamic processes in polar ocean regions. Estimates on carbon transport are very important to predict future changes of the global carbon cycle and their impact on the global climate which requires the continuous improvement and, even more important, the critical questioning of existing scientific methods."

Figures

Fig 5. and Fig. 6 are practically the same - is Fig 6 really necessary in that paper? Perhaps distinguishing between the data marks would be enough?

These figures are practically not the same since Fig. 5 points out the age ratio in general separated by water masses. Figure 6 is the basis for our assumption that the IG-TTD is valid and that the data needs corrections for saturation effects.

Fig. 7 – provides little information. In my opinion it should be more detailed (or maybe merged with subplots from Fig. 8) or removed.

We thank the reviewer for this suggestion and have now merged the two figures into one.

A few technical corrections:

Page 2194 - Section 3.8, not 3.6
corrected

Page 2197 – von Appen et al., 2015 – already published
corrected

Page 2197 – A typo in the surname Beszczynska-Möller (check in the whole paper)
corrected

Page 2199 – “at _ 200m” – should be _ not _ (also in some other cases in the paper, but not everywhere)
corrected

Page 2206 – “100 % corresponds to a anthropogenic carbon” – delete the indefinite article.
corrected

“the” Fram Strait – correct in the whole paper
corrected

Manuscript prepared for Ocean Sci.
with version 5.0 of the LaTeX class copernicus.cls.
Date: 11 January 2016

Transient tracer distributions in the Fram Strait in 2012 and inferred anthropogenic carbon content and transport

T. Stöven[1], T. Tanhua[1], M. Hoppema[2], and W.-J. von Appen[2]

[1]Helmholtz Centre for Ocean Research Kiel, GEOMAR, Germany
[2]Alfred Wegener Institute Helmholtz Centre for Polar and Marine Research, Bremerhaven, Germany

Correspondence to: T. Stöven
(tstoeven@geomar.de)

Abstract. The storage of anthropogenic carbon in the ocean's interior is an important process which modulates the increasing carbon dioxide concentrations in the atmosphere. The polar regions are expected to be net sinks for anthropogenic carbon. Transport estimates of dissolved inorganic carbon and the anthropogenic offset can thus provide information about the magnitude of the corresponding storage processes.

Here we present a transient tracer, dissolved inorganic carbon (DIC) and total alkalinity (TA) data set along $78°50'$N sampled in the Fram Strait in 2012. A theory on tracer relationships is introduced which allows for an application of the Inverse Gaussian - Transit Time Distribution (IG-TTD) at high latitudes and the estimation of anthropogenic carbon concentrations. Mean current velocity measurements along the same section from 2002-2010 were used to estimate the net flux of DIC and anthropogenic carbon by the boundary currents through the Fram Strait above 840m.

The new theory explains the differences between the theoretical (IG-TTD based) tracer age relationship and the specific tracer age relationship of the field data by saturation effects during water mass formation and / or the deliberate release experiment of SF_6 in the Greenland Sea in 1996 rather than by different mixing or ventilation processes. Based on this assumption, a maximum SF_6 excess of $0.5 - 0.8\,fmol\,kg^{-1}$ was determined in the Fram Strait at intermediate depths ($500\,m$ - $1600\,m$). The anthropogenic carbon concentrations are $50 - 55\,\mu mol\,kg^{-1}$ in the Atlantic Water / Recirculating Atlantic Water, $40 - 45\,\mu mol\,kg^{-1}$ in the Polar Surface Water / warm Polar Surface Water and between $10 - 35\,\mu mol\,kg^{-1}$ in the deeper water layers, with lowest concentrations in the bottom layer. The net fluxes through the Fram Strait indicate a net outflow of $\sim 0.4\,PgC\,yr^{-1}$ DIC and $\sim 0.01\,PgC\,yr^{-1}$ anthropogenic carbon from the Arctic Ocean into the North Atlantic, albeit with high uncertainties.

1 Introduction

Changes in the Arctic during the last decades stand in mutual relationship with changes in the adjacent ocean areas such as the Nordic Seas, the Atlantic and the Pacific Ocean. The temperature of the Atlantic Water flowing into the Arctic Ocean through the Fram Strait has warmed since 1997 (Beszczynska-Möller et al., 2012), which thus increased the heat flux into the Arctic. This has a significant influence on the perennial sea ice thickness and volume and thus on the fresh water budget (Polyakov et al., 2005; Stroeve et al., 2008; Kwok et al., 2009; Kurtz et al., 2011). The exchange and transport of heat, salt and fresh water through the major gateways like the Fram Strait, Barents Sea Opening, Canadian Archipelago and Bering Strait are also directly related to changes in ventilation of the adjacent ocean areas (Wadley and Bigg, 2002; Vellinga et al., 2008; Rudels et al., 2012). The ventilation processes of the Arctic Ocean have a significant impact on the anthropogenic carbon storage in the world ocean (Tanhua et al., 2008). Studying the fluxes of anthropogenic carbon through the major gateways contributes to understand the integrated magnitude of such ocean-atmosphere interactions. It additionally provides information of a changing environment in the Arctic Mediterranean. The required flux data of the prevailing water masses, i.e. current velocity fields, are obtained by time series of long-term maintained mooring arrays in the different gateways. The Fram Strait is the deepest gateway to the Arctic Ocean with highest volume fluxes equatorwards and polewards. A well-established cross-section mooring array is located at $\sim 78°50'$N in the Fram Strait (Fahrbach et al., 2001;

Schauer et al., 2008) which provided the basis for heat transport estimates in the past (Fahrbach et al., 2001; Schauer et al., 2004, 2008; Beszczynska-Möller et al., 2012). However, the current data interpretation and analysis of this mooring array is complicated due to a recirculation pattern in the Fram Strait (Schauer and Beszczynska-Möller, 2009; Rudels et al., 2008; Marnela et al., 2013; de Steur et al., 2014) and strong mesoscale eddy activity (von Appen et al., 2015a). The spatial and temporal volume flux variability and the insufficient instrument coverage in the deeper water layers, i.e. below the West Spitsbergen Current (WSC) and East Greenland Current (EGC), lead to high uncertainties of the net flux through the Fram Strait. Hence, it is the most relevant but also the most challenging gateway with respect to transport budgets in the Arctic Mediterranean.

Estimating an anthropogenic carbon budget presupposes the knowledge of the concentration ratio between the natural dissolved inorganic carbon (DIC) and the anthropogenic part (C_{ant}) in the water column. An estimate of DIC transport across the Arctic Ocean boundaries is provided by MacGilchrist et al. (2014) who used velocity fields by Tsubouchi et al. (2012) and available DIC data. That work provides a proper estimate of DIC fluxes, although it does not separate the specfic share of anthropogenic carbon and the uncertainties are relatively high. Similarly, Jeansson et al. (2011) calculated fluxes of inorganic, organic and anthropogenic carbon to the Nordic Seas using an extensive set of carbon and transient tracer data. Here we present anthropogenic carbon column inventories in the Fram Strait using a new data set of SF_6 and CFC-12 along the cross-section of the mooring array at 78°50′N. The anthropogenic carbon column inventories were estimated using the transient tracers and the Inverse Gaussian transit time distribution (IG-TTD) model. Flux estimates of DIC and anthropogenic carbon including the Atlantic Water, Recirculating Atlantic Water, Arctic Atlantic Water and Polar Water water masses through the Fram Strait above $840\,m$ are provided based on mean velocities measured with moorings between 2002 and 2010. Common error sources and specific aspects using these tracers and method in the Fram Strait are highlighted.

2 Material and Methods

2.1 Tracer and carbon data

A data set of CFC-12, SF_6, DIC and TA was obtained during the ARK-XXVII/1 expedition from 14 June to 15 July 2012 from Bremerhaven, Germany to Longyearbyen, Svalbard on the German research vessel *Polarstern* (Beszczynska-Möller, 2013). Figure 1 shows the stations of the zonal section along 78°50′N, where measurements of CFC-12, SF_6, DIC, and TA were conducted. The meridional section along the fast ice edge was only sampled for CFC-12 and SF_6 and shows no differences in the horizontal tracer distributions compared to the corresponding longitude range of the zonal section. Therefore we have only used the zonal section for the following analysis.

Water samples for the determination of the transient tracers CFC-12 and SF_6 were taken with $250\,ml$ glass syringes and directly measured on board, using a purge and trap GC-ECD system similar to Law et al. (1994) and Bullister and Wisegarver (2008). The measurement system is identical to the "PT3" system described in Stöven and Tanhua (2014) except the cooling system and column composition. The trap consisted of a 1/16" column packed with 70 cm *Heysep D* and cooled to −70°C during the purge process using a Dewar filled with a thin layer of liquid nitrogen. The 1/8" precolumn was packed with 30 cm *Porasil C* and 60 cm *Molsieve 5 Å* and the 1/8" main column with 180 cm *Carbograph 1AC*. Due to malfunctioning of the Electron Capture Detector (ECD) of the measurement system, the samples of 6 stations (between station 15 and 53) were taken with $300\,ml$ glass ampules and flame sealed for later onshore measurements at GEOMAR. The onshore measurement procedure is described in Stöven and Tanhua (2014). The precision for the onshore measurements is $\pm 4.4\,\%/0.09\,fmol\,kg^{-1}$ for SF_6 and $\pm 1.9\,\%/0.09\,pmol\,kg^{-1}$ for CFC-12. The precision for onboard measurements is $\pm 0.5\,\%/0.02\,fmol\,kg^{-1}$ for SF_6 and $\pm 0.6\,\%/0.02\,pmol\,kg^{-1}$ for CFC-12.

Water samples for DIC and total alkalinity (TA) were taken with $500\,ml$ glass bottles and poisoned with $100\,\mu l$ of a saturated mercuric chloride solution to prevent biological activities during storage time. The sampling procedure was carried out according to Dickson et al. (2007). The measurements of DIC and TA were performed onshore at the GEOMAR, using a coulometric measurement system (SOMMA) for DIC (Johnson et al., 1993, 1998) and a potentiometric titration (VINDTA) for TA (Mintrop et al., 2000). The precision is $\pm 0.05\,\%/1.1\,\mu mol\,kg^{-1}$ for DIC and $\pm 0.08\,\%/1.7\,\mu mol\,kg^{-1}$ for TA. The data of all obtained chemical parameters will be available at the Carbon Dioxide Information Analysis Center (CDIAC) by the beginning of 2016. The physical oceanographic data (temperature, salinity, and pressure) from this cruise can be found at Beszczynska-Möller and Wisotzki (2012).

2.2 Water transport data

An array of moorings across the deep Fram Strait from 9°E to 7°W has been maintained since 1997 by the Alfred Wegener Institute and the Norwegian Polar Institute. Since 2002, it has contained 17 moorings at 78°50′N. Here we use the gridded data from the array from summer 2002 to summer 2010 as described in Beszczynska-Möller et al. (2012). The more recent data has either not been recovered yet or the processing is still in progress. The moorings contained temperature and velocity sensors at five standard depths: $75\,m$, $250\,m$, $750\,m$, $1500\,m$, and $10\,m$ above the bottom. The hourly measurements were averaged to monthly values and then grid-

ded onto a regular $5\,m$ vertical by $1000\,m$ horizontal grid using optimal interpolation. While the Atlantic Water in Fram Strait has warmed since 1997, Beszczynska-Möller et al. (2012) showed that there is a strong seasonal cycle in the Atlantic Water transport through the Fram Strait, but that there is no statistically significant interannual trend between 1997 and 2010 in the volume transport. We consider the long term average volume flux of the following water masses: Atlantic Water advected in the West Spitsbergen Current defined as longitude $\geq 5°$E and depth $\leq 840\,m$; Polar Water flowing southward in the East Greenland Current defined as mean temperature $\leq 1°C$ and depth $\leq 400\,m$; and finally Recirculating and Arctic Atlantic Water which is both due to the recirculation of Atlantic Water in the Fram Strait (de Steur et al., 2014) and the long loop of Atlantic Water through the Arctic Ocean (Karcher et al., 2012), defined as longitude $\leq 1°$E and depth $\leq 840\,m$, not Polar Water. The estimate of the volume transport across the Fram Strait below $840\,m$ from the moorings is more complicated. The method of Beszczynska-Möller et al. (2012) which was developed to study the fluxes in the West Spitsbergen Current predicts a net southward transport of $3.2\,Sv$ below $840\,m$. This is unrealistic given that there are no connections between the Nordic Seas and the Arctic Ocean below the sill depth of the Greenland-Scotland Ridge ($840\,m$) other than the Fram Strait. No vertical displacements of isopycnals in these two basins are observed that would suggest a non-zero net transport across the Fram Strait below $840\,m$ (von Appen et al., 2015b). The large net transport inferred by Beszczynska-Möller et al. (2012) is due to the insufficient horizontal resolution of the mooring array to explicitly resolve the westward flow of the recirculation and the mesoscale eddies. For these reasons we assume a net flux of $0\,Sv$ across the Fram Strait for the deep waters below $840\,m$.

2.3 TTD method

A transit time distribution (TTD) model (Eq. 1) describes the propagation of a boundary condition into the interior of the ocean and is based on the Green's function (Hall and Plumb, 1994).

$$c(t_s,r) = \int_0^\infty c_0(t_s-t)e^{-\lambda t}\cdot G(t,r)dt \qquad (1)$$

Here, $c(t_s,r)$ is the specific tracer concentration at year t_s and location r, $c_0(t_s-t)$ the boundary condition described by the tracer concentration at source year t_s-t and $G(t)$ the transit time distribution of the tracer. The exponential term corrects for the decay rate of radioactive transient tracers. Equation 2 provides a possible solution of the TTD model, based on a steady and one-dimensional advective velocity and diffusion gradient (Waugh et al., 2003).

$$G(t) = \sqrt{\frac{\Gamma^3}{4\pi\Delta^2 t^3}}\cdot exp\left(\frac{-\Gamma(t-\Gamma)^2}{4\Delta^2 t}\right) \qquad (2)$$

It is known as the Inverse-Gaussian transit time distribution (IG-TTD) where $G(t)$ is defined by the width of the distribution (Δ), the mean age (Γ) and the time range (t). One can define a Δ/Γ ratio of the IG-TTD which represents the proportion between the advective and diffusive properties of the mixing processes as included in the TTD. The lower the Δ/Γ ratio, the higher is the advective share. A Δ/Γ ratio of 1.0 is the commonly applied ratio (unity ratio) at several tracer surveys (e.g. Waugh et al., 2004, 2006; Tanhua et al., 2008; Schneider et al., 2010; Huhn et al., 2013; Schneider et al., 2014).

Another approach is based on a linear combination of two IG-TTDs which can be used to describe more complex ventilation patterns (Eq. 3) (Waugh et al., 2002). The variables of this model are $\Delta_{1,2}$ and $\Gamma_{1,2}$ of the two IG-TTDs and α which describes the ratio between both distributions. The main problem of applying this method is that five free parameters need to be determined. Hence, this model combination can be constrained with five transient tracers with sufficiently different input functions. Alternatively, predefined parameters can be used (Stöven and Tanhua, 2014).

$$c(t_s,r) = \int_0^\infty c_0(t_s-t)e^{-\lambda t}\cdot$$

$$[\alpha\, G(\Gamma_1,\Delta_1,t,r) + (1-\alpha)\, G(\Gamma_2,\Delta_2,t,r)]\,dt \qquad (3)$$

Note that the use of CFC-12 as transient tracer is limited to concentrations below the recent atmospheric level since the production of CFC-12 was phased out in the early 1990s so that the depletion rate exceeds the emission rate since the early 2000s. This causes indistinct time information of CFC-12 since one concentration describes two dates in the atmospheric history. To this end, the use of CFC-12 is restricted to water masses with concentrations below the current atmospheric concentration limit. The emission rate of SF_6 still exceeds the depletion rate so that the atmospheric concentration is still increasing. SF_6 thus provides distinct age information of water masses over the complete concentration range.

2.4 Anthropogenic carbon and transport estimates

The IG-TTD model can be used to estimate the total amount of anthropogenic carbon in the water column (Waugh et al., 2004). For this purpose it is assumed that the anthropogenic carbon behaves like an inert passive tracer, i.e. similar to a transient tracer. Then applying equation 1, the concentration

of anthropogenic carbon in the interior ocean ($C_{ant}(t_s)$) is given by equation 4.

$$C_{ant}(t_s) = \int_{\infty}^{0} C_{ant,0}(t_s - t) \cdot G(r,t)dt \quad (4)$$

$C_{ant,0}$ is the boundary condition of anthropogenic carbon at year $t_s - t$ and $G(r,t)$ the distribution function (see equation 1). The historic boundary conditions are described by the differences between the preindustrial and modern DIC concentrations at the ocean surface. These anthropogenic offsets can be calculated by applying the modern (elevated) partial pressures of CO_2 and then subtracting the corresponding value of the preindustrial partial pressure. In each case, the preformed alkalinity was used as second parameter to determine the specific DIC concentrations (calculated using the Matlab version of the CO2SYS (van Heuven et al., 2011)). Here we assumed a constant $pCO_{2,water}$ saturation in the surface. Since exact saturations are not well constrained, we present sensitivity calculations of different saturation states / disequilibria (see section 3.6 below). The atmospheric history of $pCO_{2,atm}$ is taken from Tans and Keeling (2015). The preformed alkalinity was determined by using the alkalinity / salinity relationship of MacGilchrist et al. (2014). This relationship is based on surface alkalinity and salinity measurements in the the Fram Strait which were corrected for sea-ice melt and formation processes.

The time-dependent boundary conditions ($C_{ant,0}$) and Eq. 4 can then be used to calculate anthropogenic carbon concentrations ($C_{ant}(t_s)$) and the corresponding mean age. Finally, the mean age of Eq. 4 can be set in relation to the transient tracer based mean age of the water and allows for back-calculating $C_{ant}(t_s)$, i.e. it provides the link between the tracer concentration and the anthropogenic carbon concentration.

We then proceed to estimate transports of anthropogenic carbon through the Fram Strait. Transports are the product of concentrations times velocities integrated over an area. We assume that the trace gas concentrations change relatively slowly between years and that there are no significant seasonal changes. Hence, we can take the concentrations from summer 2012 to be informative about other seasons and years within some range from 2012. On the other hand, it is known that velocities change strongly between seasons (and on shorter time scales), but on average not significantly between years in the Fram Strait (Beszczynska-Möller et al., 2012). It follows that the measured (2002-2010) long term average volume transport is representative of the volume transport through the Fram Strait in the late 2000s/early 2010s. Likewise, the measured Cant concentrations in summer 2012 are representative for the Cant concentrations in the late 2000s/early 2010s. The product of the two is then our estimate of the Cant transport through the Fram Strait in the late 2000s/early 2010s.

3 Results and Discussion

3.1 Water masses in the Fram Strait

To highlight the different transient tracer characteristics we defined the water mass type of each sample by using the water mass properties suggested by Rudels et al. (2000, 2005) and the salinity and temperature data of this cruise from Beszczynska-Möller and Wisotzki (2012).

Water masses of the Arctic Ocean are the Polar Surface Water (PSW) which is the cold and low saline surface and halocline water; the warm Polar Surface Water, defined by a potential temperature (Θ) > 0, which comprises sea ice melt water due to interaction with warm Atlantic Water and due to solar radiation; the Arctic Atlantic Water which derives from sinking Atlantic Water due to cooling in the Arctic Ocean. The deep water masses are upper Polar Deep Water (uPDW), Canadian Basin Deep Water (CBDW) and Eurasian Basin Deep Water (EBDW). Deep water formation, e.g. on the Arctic shelves, usually involves densification due to brine rejection. The Eurasian Basin Deep Water mixes with Greenland Sea Deep Water so that this layer corresponds to two sources in the Fram Strait (von Appen et al., 2015b).

Water masses of the Atlantic Ocean / Nordic Seas are the warm and saline Atlantic Water (AW) and the corresponding Recirculating Atlantic Water (RAW); the Arctic Intermediate Water (AIW) which is mainly formed in the Greenland Sea; the Nordic Seas Deep Water (NDW) which comprises Greenland Sea Deep Water (GSDW), Iceland Sea Deep Water (ISDW) and Norwegian Sea Deep Water (NSDW) and is formed by deep convection during winter time.

Figure 2 shows the zonal water mass distribution in the Fram Strait based on salinity and temperature data from the CTD. The surface layer is dominated by Atlantic Water and Recirculating Atlantic Water in the east and by Polar Surface Water in the west with a transition between $6°$W and $4°$E where Polar Surface Water overlays the Atlantic Water. Warm Polar Surface Water can be found within the Atlantic Water between $4 - 8°$E. The Atlantic Water layer extends down to $\sim 600\,m$. Arctic Atlantic Water can be found at the upper continental slope of Greenland between $300 - 700\,m$. The intermediate layer between $500 - 1600\,m$ consists mainly of Arctic Intermediate Water and, at the Greenland slope, partly of Upper Polar Deep Water. Canadian Basin Deep Water can be found between $1600 - 2400\,m$ west of $4°$E. Nordic Seas Deep Water is the prevailing water mass along the continental slope of Svalbard between $700 - 2400\,m$ but can be also observed in the range of the Canadian Basin Deep Water layer. The Eurasian Basin Deep Water / Greenland Sea Deep Water forms the bottom layer below $2400\,m$.

3.2 Transient tracer and DIC distributions

Figure 3 shows the partial pressure of CFC-12 and SF_6 at the zonal section across the Fram Strait. Both tracers have

significant concentrations through the entire water column and show a similar distribution pattern. The Atlantic Water shows a relatively homogeneous distribution of both tracers with CFC-12 partial pressures $> 450\,ppt$ and SF_6 $> 6\,ppt$. The Polar Surface Water at the shelf region shows a more distinct structure with partial pressures between $4-8\,ppt$ of SF_6 and $410-560\,ppt$ of CFC-12. The smaller concentration gradient of CFC-12 in the surface compared to SF_6 is related to the recently decreasing atmospheric concentration of CFC-12, which causes only slightly varying boundary conditions at the air-sea interface (see section 2.3). The high-tracer concentration layer of the Polar Surface Water extends further eastwards as overlaying tongue of the Atlantic Water between $2-6°$W. The intermediate layer between $500-1600\,m$ is characterized by a clear tracer minimum along the continental slope of Greenland with partial pressures between $1.8-4.0\,ppt$ of SF_6 and $150-350\,ppt$ of CFC-12 and mainly comprises Arctic Atlantic Water. East of this minimum, a remarkable tracer maximum can be observed at $1-3°$W with partial pressures between $3-6\,ppt$ of SF_6 and $250-450\,ppt$ of CFC-12. A smaller maximum can be observed between $5-6°$E at $\sim 1000\,m$ with partial pressures of $\sim 5\,ppt$ of SF_6 and $\sim 330\,ppt$ of CFC-12. Both tracer maxima probably correspond to recently ventilated water which mainly affected the Arctic Intermediate Water and partly the Atlantic Water in the transition zone of both water masses. The Arctic Intermediate Water in the Fram Strait thus consists of recently ventilated areas and less ventilated areas which is also indicated by the large range of transient tracer concentrations. The remaining intermediate layer above $1700\,m$ is characterized by lower partial pressures between $2-3\,ppt$ of SF_6 and $150-300\,ppt$ of CFC-12 with decreasing concentrations with depth. This gradient extends throughout the deep water layers down to the bottom with partial pressures from $2\,ppt$ down to $0.2\,ppt$ of SF_6 and from $150\,ppt$ down to $34\,ppt$ of CFC-12.

Figure 4 shows the DIC concentrations along the zonal section. The Greenland shelf region shows concentrations between $1970\,\mu mol\,kg^{-1}$ in the surface and $2145\,\mu mol\,kg^{-1}$ at $\sim 200\,m$. The upper $200\,m$ between $4-8°$E shows increasing concentrations with depth between $2070\,\mu mol\,kg^{-1}$ and $2155\,\mu mol\,kg^{-1}$. There are three significant DIC maxima below $200\,m$. Two are located at the continental slope of Svalbard at $300-800\,m$ and at $1400-2100\,m$ with concentrations $> 2158\,\mu mol\,kg^{-1}$ and a maximum concentration of $2167\,\mu mol\,kg^{-1}$. The third maximum corresponds to the transient tracer maximum at $1-3°$W but extends further eastwards with concentrations between $2158\,\mu mol\,kg^{-1}$ and $2162\,\mu mol\,kg^{-1}$. The area of the East Greenland Current at $3-8°$W is characterized by concentrations between $2118\,\mu mol\,kg^{-1}$ and $2152\,\mu mol\,kg^{-1}$. The deep water below $1700\,m$ shows concentrations between $2150\,\mu mol\,kg^{-1}$ and $2158\,\mu mol\,kg^{-1}$.

3.3 Transient tracers and the IG-TTD

The IG-TTD can be numerically constrained using transient tracer couples, CFC-12 and SF_6 in our case, which provides information about the mean age and the parameters of the IG-TTD (Waugh et al., 2002; Sonnerup et al., 2013; Stöven and Tanhua, 2014). The method of validity areas, introduced in Stöven et al. (2015), is used to determine the applicability of the tracer couple. For this purpose, the tracer age is calculated from the transient tracer concentrations (Waugh et al., 2003) which provides the tracer age relationship of the tracer couple. Figure 5 shows the tracer age relationship of our field data (colored by water mass) in relation to the range of theoretical tracer age relationships of the IG-TTD, i.e. for Δ/Γ ratios between $0.1-1.8$, which describe the range from advectively dominated to diffusively dominated water masses (grey shaded area). The black line in Fig. 5 denotes the tracer age relationship based on the unity ratio of $\Delta/\Gamma = 1.0$. Field data which corresponds to this unity ratio would be centered around the black line.

The Fram Strait data can generally be separated into two sets of tracer age relationships. The upper set consists of water masses of Atlantic origin and deep waters, namely Atlantic Water / Recirculating Atlantic Water, Arctic Intermediate Water, Nordic Seas Deep Water, Eurasian Basin Deep Water / Greenland Sea Deep Water and Canadian Basin Deep Water whereas the lower set only consists of water masses of polar origin, namely Polar Surface Water, warm Polar Surface Water, Arctic Atlantic Water and upper Polar Deep Water. Note that the Arctic Atlantic Water and upper Polar Deep Water merge with the upper set for SF_6 tracer age larger than about 25 years. However, the upper set does not correspond to the unity ratio and, moreover, it is outside the validity area of the IG-TTD. Water masses related to the lower set can be applied to the IG-TTD with tendencies towards higher Δ/Γ ratios (> 1.0) since the data is clearly above the black line indicating a dominance of diffusive processes.

Another approach is provided by the linear combination of two IG-TTDs. Since we only have the data of two transient tracers, we used the same predefined parameters as described in Stöven and Tanhua (2014) which includes one more diffusive water parcel ($\Delta_1/\Gamma_1 = 1.4$) and one very advective water parcel ($\Delta_2/\Gamma_2 = 0.6$). Figure 6 shows, similar to Fig. 5, the validity area of the linear combination of two IG-TTDs for different α of 0.2, 0.5 and 0.8. Although this combination describes several scenarios from highly advective to diffusive mixing of two distributions, it can be seen that most of the observed data points are still outside the validity area. Thus, the tracer age relationship between CFC-12 and SF_6 can neither be described by the IG-TTD nor a linear combination of two IG-TTDs.

Based on the raw field data, and on assumptions implemented in the IG-TTD (like constant mixing processes along the flow pathway as well as constant saturation of the gases at the surface before entering deeper layers), the IG-TTD or lin-

ear combinations of the IG-TTD can only partly describe the ventilation pattern of water masses in the Fram Strait. Nevertheless, by comparing the shape of the two field data sets with the shape of the black line in Fig. 5, it is noted that both sets show similar characteristics as the unity ratio or, generally, as IG-TTD based tracer age relationships. This opens up the possibility to use the IG-TTD the other way around, i.e. to assume a fixed Δ/Γ ratio to determine the deviation of transient tracer concentrations rather than using the transient tracer concentration to determine the Δ/Γ ratio. Since several publications found the unity ratio of $\Delta/\Gamma = 1.0$ to be valid in large parts of the ocean, we assumed that this is also true for water masses in the Fram Strait. Figure 7 shows the mean tracer age relationship of the upper set (red line) and the tracer age relationship of the unity ratio (black line / same as in Fig. 5). The offset of the field data related to the unity ratio suggests an undersaturation of CFC-12 and / or a supersaturation of SF_6 (see black box in Fig. 7). This uncommon coexistence of under- and supersaturated transient tracers is discussed in the following section.

3.4 Saturations and excess SF_6

The surface saturations of transient tracers are influenced by sea surface temperature and salinity, ice coverage, wind speed, bubble effects, atmospheric growth rate of the tracer and the boundary dwell time of the water parcel (i.e. the time the water parcel is in contact with the atmosphere). However, the saturation state of transient tracers at the air-sea interface before, during and after water mass formation is rarely known, since water mass formation generally occurs in winter at high latitudes, which renders it almost impossible to obtain measurements. Shao et al. (2013) provide modelled data of monthly surface saturations of CFC-11, CFC-12 and SF_6 from 1936 to 2010 on a global scale. This model output can be used to estimate the tracer saturation ratio of different water masses by using the surface saturation of the specific formation area and yearly formation period. The formation types and areas are notably different for water masses that occur in the Fram Strait. The model output shows high variabilities in surface saturations at different formation sites, namely the Greenland Sea, the Arctic shelf regions and the Arctic open water (Fig. 8). In contrast, the tracer age relationships of the two sets in Fig. 5 indicate relatively similar deviations in saturation. The complex boundary conditions in the Arctic, e.g. possible gas exchange through ice cover and the changing extent of the ice cover, might bias the results of the saturation model. Therefore, we only used the surface saturation of the Greenland Sea (Area 1 in Fig. 8) which agrees with the findings of Tanhua et al. (2008) who used available field data to investigate historic tracer saturations. The IG-TTD based mean age provides the link between the observed tracer concentrations and the corresponding time-dependent saturation. Therefore, the saturation corrections were applied to the atmospheric history (boundary conditions) of each tracer. These new boundary conditions are then applied to the measured tracer concentrations and the IG-TTD which then yields a saturation-corrected mean age. This mean age in turn can then be used to back-calculate the saturation-corrected tracer concentrations using the original (uncorrected) boundary conditions.

The SF_6 excess is estimated using the corrected CFC-12 concentrations and the IG-TTD ($\Delta/\Gamma = 1.0$) to calculate theoretical SF_6 concentrations of the water parcel, i.e. back-calculated SF_6 concentrations. The difference between the theoretical SF_6 concentration and the measured SF_6 concentration denotes the SF_6 excess in the water. Note that this SF_6 excess is based on the assumption that the IG-TTD and unity ratio describe the prevailing ventilation pattern of the water masses. Figure 9 shows the SF_6 excess in $fmol\,kg^{-1}$ and ppt for depths below $200\,m$. This upper depth limit is invoked by the fact that CFC-12 concentrations above the current atmospheric concentration limit cannot be applied to the IG-TTD. The SF_6 excess is much higher ($0.5-0.8\,fmol\,kg^{-1}$ / $1.0-1.6\,ppt$) for northwards propagating water masses compared to water masses of Arctic origin ($0-0.4\,fmol\,kg^{-1}$ / $0-0.8\,ppt$). There are at least two possible effects which can cause such significant supersaturations of SF_6.

One possibility refers to the deliberate tracer release experiment in 1996 where $320\,kg$ ($\sim 2190\,mol$) of SF_6 were introduced into the central Greenland Sea (Watson et al., 1999). The patch was redistributed by mixing processes and entered the Arctic Ocean via the Fram Strait and Barents Sea Opening and the North Atlantic via Denmark Strait and the Faroe Bank Channel (Olsson et al., 2005; Tanhua et al., 2005; Marnela et al., 2007). Assuming that $50-80$ % of the deliberatly released SF_6 still remains in the Nordic Seas and the Arctic Ocean ($1095-1752\,mol$) and that $10-50$ % of the corresponding total water volume of $1.875\cdot10^{18}-9.375\cdot10^{18}\,l$ (Eakins and Sharman, 2010) is affected, a mean offset of $0.12-0.93\,fmol\,l^{-1}$ might be found. This mean offset is in the range of the observed SF_6 excess concentrations. However, CFC-12 and SF_6 data of the Southern Ocean (Stöven et al., 2015) shows similar tracer age relationships compared to the Fram Strait data but with no influence of deliberately released SF_6. This indicates that another source of excess SF_6 may exists which is much larger than the source of the tracer release experiment.

Liang et al. (2013) introduced a model which estimates supersaturations of dissolved gases by bubble effects in the ocean. This model predicted an increasing supersaturation for increasing wind speed and decreasing temperature, i.e. the bubble effect becomes more significant at high latitudes. Furthermore, Liang et al. (2013) show that the magnitude of supersaturation depends on the solubility of the gas. The less soluble a gas, the more supersaturation can be expected. Supporting this, Stöven et al. (2015) describe surface measurements of SF_6 and CFC-12 directly after heavy wind conditions in the Southern Ocean where SF_6 supersaturations of $20-50$ % could be observed. The CFC-12 concentrations

were only affected to a minor extent which indeed can be explained by the differences in solubility. This bubble-induced supersaturation can also be expected to occur during the process of water mass formation in the Greenland Sea which usually occurs during late winter, i.e. during a period with low surface temperatures and heavy wind conditions. Furthermore, the maximum SF_6 excess in the Arctic Intermediate Water layer in Fig. 9 and the generally elevated tracer concentrations of CFC-12 and SF_6 in the same area (see Fig. 3) reaffirm the assumption of bubble induced supersaturation of SF_6. However, this hypothesis stands in opposition to the current assumption that trace gases are generally undersaturated during water mass formation (Tanhua et al., 2008; Shao et al., 2013).

Future investigations are necessary to determine the different impact of under- and supersaturation effects on soluble gases at the air-sea interface. It can be expected that possible scenarios are not restricted to distinct saturation states anymore but rather comprise mixtures of equilibrated, under- and supersaturated states of the different gases.

3.5 Anthropogenic carbon and mean age

Since CFC-12 is not affected by tracer release experiments and possibly only to minor extent by bubble effects we used this tracer to calculate the mean age of the water and the corresponding anthropogenic carbon content. SF_6 was only used in the surface and upper halocline, i.e. where CFC-12 exceeds the atmospheric concentration limit of $528\,ppt$ and where effects of SF_6 supersaturation are comparatively small. Saturation-corrected tracer data was applied for subsurface data below $100\,m$ whereas surface data was found to be near equilibrium state with the atmosphere. Figure 10 shows the anthropogenic carbon distribution and Fig. 11 shows the mean age of the water masses. As expected from the relation between transient tracers, mean age and anthropogenic carbon, the distribution patterns are similar to that of transient tracers. The highest anthropogenic carbon concentrations of $50-55\,\mu mol\,kg^{-1}$ were found in the upper $600\,m$ of the Atlantic Water / Recirculating Atlantic Water and slightly lower concentrations of $40-45\,\mu mol\,kg^{-1}$ in the Polar Surface Water / warm Polar Surface Water layer. The mean age of these water masses is $0-20$ years. Note that these water layers show the highest mean current velocities in the Fram Strait (see section 3.7 below). The area of the tracer maximum at $1-3°$W shows elevated concentrations of $35-40\,\mu mol\,kg^{-1}$ and a mean age of $20-40$ years. The remaining water layers below $600\,m$ show anthropogenic carbon concentrations lower than $35\,\mu mol\,kg^{-1}$ with decreasing concentrations with increasing depth; anthropogenic carbon is comparatively low ($<10\,\mu mol\,kg^{-1}$) in deep water masses such as Canadian Basin Deep Water and Eurasian Basin Deep Water / Greenland Sea Deep Water. Accordingly, the mean age increases with increasing depth from 30 years to 280 years and shows a maximum mean age of 286 years in the bottom layer at the prime meridian. Table 1 shows the mean values and standard deviation of each specific water layer.

The determined values are comparable to the findings of Jutterström and Jeansson (2008) who used a similar method to determine anthropogenic carbon of the East Greenland Current in 2002. The Fram Strait section of their data set shows a similar distribution pattern of anthropogenic carbon but with lower concentration levels compared to our data from 2012. The concentration differences indicate an increase of the anthropogenic carbon content between $25-35$ % in the entire water column during the elapsed ten years. This corresponds to an increase of $2\,\mu mol\,kg^{-1}\,yr^{-1}$ in the Atlantic Water, $1\,\mu mol\,kg^{-1}\,yr^{-1}$ in the Polar Water and between $0.5-1\,\mu mol\,kg^{-1}\,yr^{-1}$ in the deeper water layers. Based on these current rates of increase it can be assumed that the import of anthropogenic carbon by Atlantic Water becomes more dominant compared to the export by Polar Water in the future. Furthermore, when looking at the different gateways to the Arctic Ocean, it can be assumed that the Atlantic Water entering the Arctic Ocean via the Barent Sea has similar anthropogenic carbon concentrations as in the Fram Strait and that the outflow water through the Canadian Archipelago has similar concentrations as the Polar Water in the Fram Strait. The inflow of Pacific Water transports $\sim 46\,\mu mol\,kg^{-1}$ of anthropogenic carbon into the Arctic Ocean (Stöven, unpublished data 2014). This implies that the inflowing water masses transport more anthropogenic carbon into the Arctic Ocean than the outflowing water masses since the water mass exchange must be balanced.

3.6 Sensitivities in anthropogenic carbon

The calculations presented above are based on the ideal case of $pCO_{2,atm}$=$pCO_{2,water}$ at the sea surface before entering the ocean interior, and the assumption that the saturation correction of the tracers and the unity ratio of the IG-TTD are true for water masses in the Fram Strait. Since these three parameters involved cannot be directly determined, it is very likely that deviations from the ideal case occur. Therefore, we present the corresponding sensitivities in the following. The sensitivities are determined by changing only one parameter and keeping the others constant at ideal conditions.

Figure 12a and 12b show the sensitivities of changes in tracer saturation using the example of CFC-12 since most of the anthropogenic carbon calculations are based on this tracer. Small deviations of ± 5 % in CFC-12 saturations cause only small deviations of anthropogenic carbon concentrations of $\pm 1\,\mu mol\,kg^{-1}$ / $\pm 2-4$ %. Furthermore, the sensitivity depends on the partial pressure range of CFC-12. The lower the partial pressure the less sensitive are the anthropogenic carbon concentrations to changes in CFC-12 saturation. The maximum deviations are $\pm 6\,\mu mol\,kg^{-1}$ / $\pm 11-16$ % for partial pressure $> 400\,ppt$. The white patches in Fig. 12a and 12b correspond to supersaturations which exceed the atmo-

spheric concentration limit of CFC-12.

Figure 12c and 12d show the sensitivities due to changes in the Δ/Γ-ratio of the IG-TTD. The sensitivity is very low ($< 1\,\mu mol\,kg^{-1}$ / < 5 %) for most of the ratio and concentration range. Partial pressures below $100\,ppt$ and $\Delta/\Gamma < 0.4$ show the highest sensitivty with deviations between $5-10\,\mu mol\,kg^{-1}$ / $50-200$ %. The unusual sensitivity distribution is related to the indistinct boundary condition of CFC-12 in recent years and the distribution function of the TTD. For more detailed information, see Stöven et al. (2015). The sensitivities of deviations in pCO_2 saturations are shown in Fig. 12e and 12f. The absolute error is characterized by a relatively steady change with changing saturation states. The absolute error is more or less independent of the partial pressure of CFC-12 and leads to maximum deviations of $\pm 20-25\,\mu mol\,kg^{-1}$. The relative error ($0-200$ %) shows an increasing sensitivity of anthropogenic carbon concentrations to changes in pCO_2 saturations and decreasing CFC-12 partial pressures. Note that a negative deviation of 100 % corresponds to anthropogenic carbon concentration of $0\,\mu mol\,kg^{-1}$ which is also indicated by the turning-points where the contour lines continue parallel to the x-axis in Fig. 12e. This indicates that small uncertainties in pCO_2 saturations can cause large errors in anthropogenic carbon estimates for low tracer concentrations, i.e. for a high mean age of the water. Furthermore it is unclear to what extent the time period and type of sea ice coverage as well as the sea ice formation and melting processes bias the pCO_2 and tracer saturations at high latitudes. The uncertainty of the pCO_2 saturation remains as the largest error source although the saturation of pCO_2 and CFC-12 counteract each other.

3.7 Carbon transport estimates

Table 2 shows the transport estimates of DIC and anthropogenic carbon separated into northwards flowing (positive values) and southwards flowing (negative values) water masses. The northwards flux comprises the Atlantic Water of the West Spitsbergen Current, the southwards flux comprises the Recirculating / Return Atlantic Water and the Polar Water of the East Greenland Current. The mean flux of deep water layers below $840\,m$ was taken to be $0\,Sv$ and therefore not considered for this estimate. Furthermore, any net flux below $1500\,m$ would not change the anthropogenic carbon inventory of the Nordic Seas or the Arctic Ocean due to the homogeneous distribution of anthropogenic carbon at these depths. The depth range between $840\,m$ and $1500\,m$ might contribute to either the Arctic or the Nordic Seas reservoir but it is still an enclosed basin-basin interaction.

The northwards flux transports $3592 \pm 2612\,TgC\,yr^{-1}$ (mean $\pm$ standard deviation) of DIC and $78 \pm 57\,TgC\,yr^{-1}$ of anthropogenic carbon into the Arctic Ocean. This inflow is exceeded by an outflow of $2852 \pm 1549\,TgC\,yr^{-1}$ / $67 \pm 36\,TgC\,yr^{-1}$ by Recirculating and Return Atlantic Water and $1118 \pm 639\,TgC\,yr^{-1}$ / $23 \pm 13\,TgC\,yr^{-1}$ by Polar Water. The carbon transport uncertainties are relatively high and there is a lack of water transport data on the Greenland shelf region, e.g. Belgica Bank. Thus we cannot with great confidence decide whether more anthropogenic carbon is transported into or out of the Arctic region through the Fram Strait.

3.8 Uncertainties

We showed that neither the IG-TTD nor linear combinations of the model can describe the tracer age relationships between CFC-12 and SF_6 in the Fram Strait. This means that either the models are not suitable to describe the prevailing ventilation pattern or that there are other reasons which lead to the specific concentration ratios. Here we focused on the second case which incorporates the assumptions that the tracer age relationships are related to different saturation states of the transient tracers and, furthermore, that the simple IG-TTD model can describe the ventilation processes of all water masses in the Fram Strait.

The uncertainties of our approach thus correspond to the chosen shape of the IG-TTD, i.e. the unity ratio of $\Delta/\Gamma = 1.0$, and the uncertainties of the measurement precision of the transient tracers and apparent transient tracers (see section 3.6 above). Further uncertainties are related to processes which influence the gas exchange and thus the boundary conditions of the tracers. This includes the important but yet rarely investigated impact of sea ice cover, sea ice formation and sea ice melting processes as well as bubble effects during heavy wind conditions, see discussion in section 3.6.

The flux estimates are based on transient tracer and DIC data of the ARK-XXVII/1 cruise which only show the specific distribution pattern during June / July 2012 and thus neglect any interannual variabilities of the parameters. The determination of the preformed alkalinity highly depends on the used method. Here we used the linear relationship between surface alkalinity and salinity which is a commonly used method. However, other authors recommend the use of alkalinity / salinity data from the subsurface layer (Vazquez-Rodriguez et al., 2012) or the surface temperature and salinity dependencies (Lee et al., 2006).

The transport estimates are complicated by the fact that the flow field in the Fram Strait is dominated by small scale features. The Rossby radius is $4-6\,km$ which means that the mooring spacing is only able to fully resolve the mesoscale near the shelfbreak in the West Spitsbergen Current. Otherwise, eddies may be aliased between the moorings. The velocities in the recirculation area in the center of the Fram Strait are actually mostly westward (Beszczynska-Möller et al., 2012) and thus along the mooring array line. Therefore, the meridional velocities in the center of the Fram Strait are only the small residuals of much larger zonal velocities. As a result the finite accuracy and precision of the current direction measurements has a big impact on the meridional

exchanges. Additionally, at depth the flow is topographically steered, but the topographic features are not fully resolved. Interannual variations are also neglected here, but they are small (Beszczynska-Möller et al., 2012). The exchange flow across the Fram Strait below $840\,m$ (sill depth of Greenland-Scotland ridge) is assumed to be $0\,Sv$ for the present purpose.

4 Conclusions

Measurements of the transient tracers CFC-12 and SF_6 along $78°50'$N in the Fram Strait in 2012 show specific characteristics of the different water masses. The tracer age relationship between both tracers can be separated into two major sets. One set describes the tracer age relationship of water masses of Atlantic origin as well as deep water masses, the other describes water masses of Arctic origin. We assumed that the different tracer age relationships are due to different saturation effects on the tracers during water mass formation and still existing offsets of the SF_6 concentrations caused by the deliberate tracer release experiment in the Greenland Sea in 1996. The CFC-12 data was saturation corrected by applying the model output of Shao et al. (2013). The corrected data was then used to back-calculate theoretical SF_6 data based on the IG-TTD which then provides the excess concentrations of SF_6. The largest excess concentrations of $0.5-0.8\,fmol\,kg^{-1}$ were found for the intermediate layer between $500\,m$ and $1600\,m$.

The anthropogenic carbon content was estimated using the IG-TTD and saturation-corrected CFC-12 data in the ocean interior (depths below $100\,m$) and SF_6 in the surface layer. The Atlantic Water and Recirculating Atlantic Water is characterized by anthropogenic carbon concentrations of $50-55\,\mu mol\,kg^{-1}$ and the Polar Surface Water by concentrations of $40-45\,\mu mol\,kg^{-1}$. Maximum concentrations of $35-40\,\mu mol\,kg^{-1}$ in the intermediate layer can be found at $1-3°$W. Deep water layers show decreasing concentrations with increasing depth from $35\,\mu mol\,kg^{-1}$ down to $\sim 10\,\mu mol\,kg^{-1}$. According to the different anthropogenic carbon concentrations of the fluxes through the Arctic Ocean gateways, i.e. with higher inflow concentrations than outflow concentrations, the Arctic Ocean can be considered as net carbon sink.

The transport estimates through the Fram Strait are characterized by high uncertainties so that we only focused on the boundary currents, namely the West Spitzbergen Current and East Greenland Current. The mean current velocity data obtained by a mooring-array at $78°50'$N between 2002 and 2010 suggests a mean northwards flux of $4.4\,(\pm 3.2)\,Sv$ of Atlantic Water (West Spitsbergen Current) and a mean southward flux of $3.5\,(\pm 1.9)\,Sv$ of Recirculating / Return Atlantic Water and $1.4\,(\pm 0.8)\,Sv$ of Polar Water (East Greenland Current). The net transport of anthropogenic carbon by the boundary currents is estimated to $-12\,TgC\,yr^{-1}$, i.e. a net outflow of the Arctic Ocean. However, the high uncertainties of the overall flux data in the Fram Strait inhibit any statements about dominating shares of DIC and anthropogenic exports or imports to the Arctic Ocean.

The theory of saturation effects on transient tracers requires more targeted experiments and data acquisition from high latitudes to get proven or rejected. However, this approach should not contradict the assumptions on complex ventilation pattern but should rather contribute to a better understanding and analysis of the dynamic processes in polar ocean regions. Estimates on carbon transport are very important to predict future changes in the global carbon cycle and their impact on the global climate which requires the continuous improvement and, even more important, the critical questioning of existing scientific methods.

Acknowledgements. This work was supported by the Deutsche Forschungsgemeinschaft (DFG) in the framework of the priority programme "Antarctic Research with comparative investigations in Arctic ice areas" by a grant to T. Tanhua and M. Hoppema: Carbon and transient tracers dynamics: A bi-polar view on Southern Ocean eddies and the changing Arctic Ocean (TA 317/5, HO 4680/1). Partial support to T. Tanhua and M. Hoppema was received from EU FP7 project CARBOCHANGE "Changes in carbon uptake and emissions by oceans in a changing climate" (European Community's 7th Framework Programme, grant agreement no. 264879). We are grateful to the Alfred-Wegener-Institut for participation in Polarstern cruise ARK-XXVII/1. We are happy to acknowledge the great support by the master and crew of Polarstern, the chief scientist and the scientific party. Special thanks goes to Boie Bogner for his technical support during the ARK-XXVII/1 cruise.

References

Beszczynska-Möller, A.: The expedition of the research vessel Polarstern to the Arctic in 2012 (ARK-XXVII/1), Reports on Polar and Marine Research, 660, 1–78, doi: 10.2312/BzPM_0660_2013, 2013.

Beszczynska-Möller, A. and Wisotzki, A.: Physical oceanography during POLARSTERN cruise ARK-XXVII/1, Alfred Wegener Institute, Helmholtz Center for Polar and Marine Research, Bremerhaven, doi: 10.1594/PANGAEA.801791, 2012.

Beszczynska-Möller, A., Fahrbach, E., Schauer, U., and Hansen, E.: Variability in Atlantic water temperature and transport at the entrance to the Arctic Ocean, 1997-2010, ICES J. Mar. Sci., 69, 852–863, 2012.

Bullister, J. L. and Wisegarver, D. P.: The shipboard analysis of trace levels of sulfur hexafluoride, chlorofluorocarbon-11 and chlorofluorocarbon-12 in seawater, Deep-Sea Res. I, 55, 1063 – 1074, 2008.

de Steur, L., Hansen, E., Mauritzen, C., Beszczynska-Möller, A., and Fahrbach, E.: Impact of recirculation on the East Greenland Current in Fram Strait: Results from moored current meter measurements between 1997 and 2009, Deep-Sea Res., 92, 26–40, 2014.

Dickson, A., Sabine, C., and Chrisitan, J.: Guide to Best Practices for Ocean CO_2 Measurements, 2007.

Eakins, B. W. and Sharman, G. F.: Volumes of the World's Ocean from ETOPO1, NOAA National Geophysical Data Center, http://ngdc.noaa.gov/mgg/global/etopo1_ocean_volumes.html, 2010.

Fahrbach, E., Meincke, J., Österhus, S., Rohardt, G., Schauer, U., Tverberg, V., and Verduin, J.: Direct measurements of volume transports through Fram Strait, Polar Res., 20, 217–224, doi: 10.1111/j.1751-8369.2001.tb00059.x, 2001.

Hall, T. M. and Plumb, R. A.: Age as a diagnostic of stratospheric transport, J. Geophys. Res., 99, 1059–1070, 1994.

Huhn, O., Rhein, M., Hoppema, M., and van Heuven, S.: Decline of deep and bottom water ventilation and slowing down of anthropogenic carbon storage in the Weddell Sea, 1984-2011, Deep-Sea Res. I, 76, 66–84, doi:10.1016/j.dsr.2013.01.005, 2013.

Jeansson, E., Olsen, A., Eldevik, T., Skjelvan, I., Omar, A. M., Lauvset, S. K., Nilsen, J. E., Bellerby, R. G. J., Johannessen, T., and Falck, E.: The Nordic Seas carbon budget: Sources, sinks, and uncertainties, Glob. Biogeochem. Cycle, 25, doi: 10.1029/2010GB003961, 2011.

Johnson, K. M., Wills, K. D., Butler, D. B., Johnson, W. K., and Wong, C. S.: Coulometric total carbon dioxide analysis for marine studies: maximizing the performance of an automated gas extraction system and coulometric detector, Mar. Chem., 44, 167–187, doi: 10.1016/0304-4203(93)90201-X, 1993.

Johnson, K. M., Dickson, A. G., Eischeid, G., Goyet, C., Guenther, P., Key, R. M., Millero, F. J., Purkerson, D., Sabine, C. L., Schottle, R. G., Wallace, D. W. R., Wilke, R. J., and Winn, C. D.: Coulometric total carbon dioxide analysis for marine studies: assessment of the quality of total inorganic carbon measurements made during the US Indian Ocean CO_2 Survey 1994-1996, Mar. Chem., 63, 21–37, doi: 10.1016/S0304-4203(98)00048-6, 1998.

Jutterström, S. and Jeansson, E.: Anthropogenic carbon in the East Greenland Current, Prog. Oceanogr., 78, 29–36, doi: 10.1016/j.pocean.2008.04.001, 2008.

Karcher, M., Smith, J. N., Kauker, F., Gerdes, R., and Smethie, W. M.: Recent changes in Arctic Ocean circulation revealed by iodine-129 observations and modeling, J. Geophys. Res. Oceans, 117, 2012.

Kurtz, N. T., Markus, T., Farrell, S. L., Worthen, D. L., and Boisvert, L. N.: Observations of recent Arctic sea ice volume loss and its impact on ocean-atmosphere energy exchange and ice production, J. Geophys. Res. Oceans, 116, doi: 10.1029/2010JC006235, 2011.

Kwok, R., Cunningham, G. F., Wensnahan, M., Rigor, I., Zwally, H. J., and Yi, D.: Thinning and volume loss of the Arctic Ocean sea ice cover: 2003-2008, J. Geophys. Res. Oceans, 114, doi: 10.1029/2009JC005312, 2009.

Law, C. S., Watson, A. J., and Liddicoat, M. I.: Automated vacuum analysis of sulphur hexafluoride in seawater: derivation of the atmospheric trend (1970-1993) and potential as a transient tracer, Mar. Chem., 48, 57 – 69, 1994.

Lee, K., Tong, L. T., Millero, F. J., Sabine, C. L., Dickson, A. G., Goyet, C., Park, G., Wanninkhof, R., Feely, R. A., and Key, R. M.: Global relationships of total alkalinity with salinity and temperature in surface waters of the worlds oceans, Geophys. Res. Lett., 33, doi: 10.1029/2006GL027207, 2006.

Liang, J.-H., Deutsch, C., McWilliams, J. C., Baschek, B., Sullivan, P. P., and Chiba, D.: Parameterizing bubble-mediated air-sea gas exchange and its effect on ocean ventilation, Global Biogeochem. Cycles, 27, 894–905, doi: 10.1002/gbc.20080, 2013.

MacGilchrist, G. A., Naveira Garabato, A. C., Tsubouchi, T., Bacon, S., Torres-Valdes, S., and Azetsu-Scott, K.: The Arctic Ocean carbon sink, Deep-Sea Res. I, 86, 39 – 55, doi: 10.1016/j.dsr.2014.01.002, 2014.

Marnela, M., Rudels, B., Olsson, K. A., Anderson, L. G., Jeansson, E., Torres, D. J., Messias, M.-J., Swift, J. H., and Watson, A. J.: Transports of Nordic Seas water masses and excess SF6 through Fram Strait to the Arctic Ocean, Prog. Oceanogr., 78, doi: 10.1016/j.pocean.2007.06.004., 2007.

Marnela, M., Rudels, B., Houssais, M., Beszczynska-Möller, A., and Eriksson, P. B.: Recirculation in the Fram Strait and transports of water in and north of the Fram Strait derived from CTD data, Ocean Sci., 9, 499–519, 2013.

Mintrop, L., Pérez, F. F., González-Dávila, M., Santana-Casiano, J. M., and Körtzinger, A.: Alkalinity determination by potentiometry: Intercalibration using three different methods, Ciencias Marinas, 26, 23–37, 2000.

Olsson, K. A., Jeansson, E., Tanhua, T., and Gascard, J.-C.: The East Greenland Current studied with CFCs and released sulphur hexafluoride, J. Mar. Sys., 55, 77–95, doi: 10.1016/j.jmarsys.2004.07.019, 2005.

Polyakov, I. V., Beszczynska, A., Carmack, E. C., Dmitrenko, I. A., Fahrbach, E., Frolov, I. E., Gerdes, R., Hansen, E., Holfort, J., Ivanov, V. V., Johnson, M. A., Karcher, M., Kauker, F., Morison, J., Orvik, K. A., Schauer, U., Simmons, H. L., Skagseth, Ø., Sokolov, V. T., Steele, M., Timokhov, L. A., Walsh, D., and Walsh, J. E.: One more step toward a warmer Arctic, Geophys. Res. Lett., 32, doi: 10.1029/2005GL023740, 2005.

Rudels, B., Meyer, R., Fahrbach, E., Ivanov, V. V., Österhus, S., Quadfasel, D., Schauer, U., Tverberg, V., and Woodgate, R. A.: Water mass distribution in Fram Strait and over the Yermak Plateau in summer 1997, Annales Geophysicae, 18, 687–705, doi: 10.1007/s00585-000-0687-5, 2000.

Rudels, B., Björk, G., Nilsson, J., Winsor, P., Lake, I., and Nohr, C.: The interaction between waters from the Arctic Ocean and the Nordic Seas north of Fram Strait and along the East Greenland Current: results from the Arctic Ocean-02 Oden expedition, J. Mar. Sys., 55, 1 – 30, doi: 10.1016/j.jmarsys.2004.06.008, 2005.

Rudels, B., Marnela, M., and Eriksson, P.: Constraints on estimating mass, heat and freshwater transports in the Arctic Ocean: An exercise, in: Arctic-Subarctic Ocean Fluxes, edited by Dickson, R., Meincke, J., and Rhines, P., pp. 315–341, Springer Netherlands, doi: 10.1007/978-1-4020-6774-7_14, 2008.

Rudels, B., Korhonen, M., Budéus, G., Beszczynska-Möller, A., Schauer, U., Nummelin, A., Quadfasel, D., and Valdimarsson, H.: The East Greenland Current and its impacts on the Nordic Seas: observed trends in the past decade, ICES J. Mar. Sci., 69, 841–851, doi: 10.1093/icesjms/fss079, 2012.

Schauer, U. and Beszczynska-Möller, A.: Problems with estimation and interpretation of oceanic heat transport - conceptual remarks for the case of Fram Strait in the Arctic Ocean, Ocean Science, 5, 487–494, doi: 10.5194/os-5-487-2009, 2009.

Schauer, U., Fahrbach, E., Østerhus, S., and Rohardt, G.: Arctic warming through the Fram Strait: Oceanic heat transport from 3 years of measurements, J. Geophys. Res. Oceans, 109, doi: 10.1029/2003JC001823, 2004.

Schauer, U., Beszczynska-Möller, A., Walczowski, W., Fahrbach, E., Piechura, J., and Hansen, E.: Variation of Measured Heat Flow Through the Fram Strait Between 1997 and 2006, in:

Arctic-Subarctic Ocean Fluxes, edited by Dickson, R., Meincke, J., and Rhines, P., pp. 65–85, Springer Netherlands, doi: 10.1007/978-1-4020-6774-7_4, 2008.

Schneider, A., Tanhua, T., Körtzinger, A., and Wallace, D. W. R.: High anthropogenic carbon content in the eastern Mediterranean, J. Geophys. Res., 115, doi:10.1029/2010JC006171, 2010.

Schneider, A., Tanhua, T., Roether, W., and Steinfeldt, R.: Changes in ventilation of the Mediterranean Sea during the past 25 year, Ocean Sci., 10, 1–16, doi: 10.5194/os-10-1-2014, 2014.

Shao, A. E., Mecking, S., Thompson, L., and Sonnerup, R. E.: Mixed layer saturations of CFC-11, CFC-12, and SF6 in a global isopycnal model, J. Geophys. Res. Oceans, 118, 4978–4988, doi: 10.1002/jgrc.20370, 2013.

Sonnerup, R. E., Mecking, S., and Bullister, J. L.: Transit time distributions and oxygen utilization rates in the Northeast Pacific Ocean from chlorofluorocarbons and sulfur hexafluoride, Deep Sea Res. I, 72, 61 – 71, doi: 10.1016/j.dsr.2012.10.013, 2013.

Stöven, T. and Tanhua, T.: Ventilation of the Mediterranean Sea constrained by multiple transient tracer measurements, Ocean Sci., 10, 439–457, doi: 10.5194/os-10-439-2014, 2014.

Stöven, T., Tanhua, T., Hoppema, M., and Bullister, J. L.: Perspectives of transient tracer applications and limiting cases, Ocean Sci., 11, 699–718, doi: 10.5194/os-11-699-2015, 2015.

Stroeve, J., Serreze, M., Drobot, S., Gearheard, S., Holland, M., Maslanik, J., Meier, W., and Scambos, T.: Arctic Sea Ice Extent Plummets in 2007, Eos, Transactions American Geophysical Union, 89, 13–14, doi: 10.1029/2008EO020001, 2008.

Tanhua, T., Bulsiewicz, K., and Rhein, M.: Spreading of Overflow Water from the Greenland to the Labrador Sea, Geophys. Res. Lett., 32, doi: 10.1029/2005GL0227700, 2005.

Tanhua, T., Waugh, D. W., and Wallace, D. W. R.: Use of SF_6 to estimate anthropogenic CO_2 in the upper ocean, J. Geophys. Res., 113, 2156–2202, doi:10.1029/2007JC004416, 2008.

Tans, P. and Keeling, R.: Full Mauna Loa CO_2 record, NOAA/ESRL, www.esrl.noaa.gov/gmd/ccgg/trends/, 2015.

Tsubouchi, T., Bacon, S., Naveira Garabato, A. C., Aksenov, Y., Laxon, S. W., Fahrbach, E., Beszczynska-Möller, A., Hansen, E., Lee, C. M., and Ingvaldsen, R. B.: The Arctic Ocean in summer: A quasi-synoptic inverse estimate of boundary fluxes and water mass transformation, J. Geophys. Res. Oceans, 117, doi: 10.1029/2011JC007174, 2012.

van Heuven, S., Pierrot, D., Rae, J. W. B., Lewis, E., and Wallace, D. W. R.: MATLAB Program Developed for CO2 System Calculations, Carbon Dioxide Information Analysis Center, doi: 10.3334/CDIAC/otg.CO2SYS_MATLAB_v1.1, 2011.

Vazquez-Rodriguez, M., Padin, X. A., Pardo, P. C., Rios, A. F., and Perez, F. F.: The subsurface layer reference to calculate preformed alkalinity and air-sea CO_2 disequilibrium in the Atlantic Ocean, J. Mar. Sys., 94, 52–63, 2012.

Vellinga, M., Dickson, B., and Curry, R.: The Changing View on How Freshwater Impacts the Atlantic Meridional Overturning Circulation, in: Arctic-Subarctic Ocean Fluxes, edited by Dickson, R., Meincke, J., and Rhines, P., pp. 289–313, Springer Netherlands, doi: 10.1007/978-1-4020-6774-7_13, 2008.

von Appen, W.-J., Schauer, U., Hattermann, T., and Beszczynska-Möller, A.: Seasonal cycle of mesoscale instability of the West Spitsbergen Current, J. Phys. Oceanogr., in revision, 2015a.

von Appen, W.-J., Schauer, U., Somavilla, R., Bauerfeind, E., and Beszczynska-Möller, A.: Exchange of warming deep waters across Fram Strait, Deep-Sea Res., 103, 86–100, doi: 10.1016/j.dsr.2015.06.003, 2015b.

Wadley, M. R. and Bigg, G. R.: Impact of flow through the Canadian Archipelago and Bering Strait on the North Atlantic and Arctic circulation: An ocean modelling study, Quarterly Journal of the Royal Meteorological Society, 128, 2187–2203, doi: 10.1256/qj.00.35, 2002.

Watson, A. J., Messias, M., Fogelqvist, E., van Scoy, K. A., Johannessen, T., Oliver, K. I. C., Stevens, D. P., Rey, F., Tanhua, T., Olsson, K. A., Carse, F., Simonsen, K., Ledwell, J. R., Jansen, E., Cooper, D. J., Kruepke, J. A., and Guilyardi, E.: Mixing and convection in the Greenland Sea from a tracer-release experiment, Nature, 401, 902–904, doi: 10.1038/44807, 1999.

Waugh, D. W., Vollmer, M. K., Weiss, R. F., Haine, T. W. N., and Hall, T. M.: Transit time distributions in Lake Issyk-Kul, Geophys. Res. Lett., 29, 84–1–84–4, doi:10.1029/2002GL016201, 2002.

Waugh, D. W., Hall, T. M., and Haine, T. W. N.: Relationships among tracer ages, J. Geophys. Res., 108, doi:10.1029/2002JC001325, 2003.

Waugh, D. W., Haine, T. W. N., and Hall, T. M.: Transport times and anthropogenic carbon in the subpolar North Atlantic Ocean, Deep Sea Res. I, 51, 1475 – 1491, 2004.

Waugh, D. W., Hall, T. M., McNeil, B. I., Key, R., and Matear, R. J.: Anthropogenic CO_2 in the oceans estimated using transit time distributions, Tellus Ser. B, 58, 376 – 389, 2006.

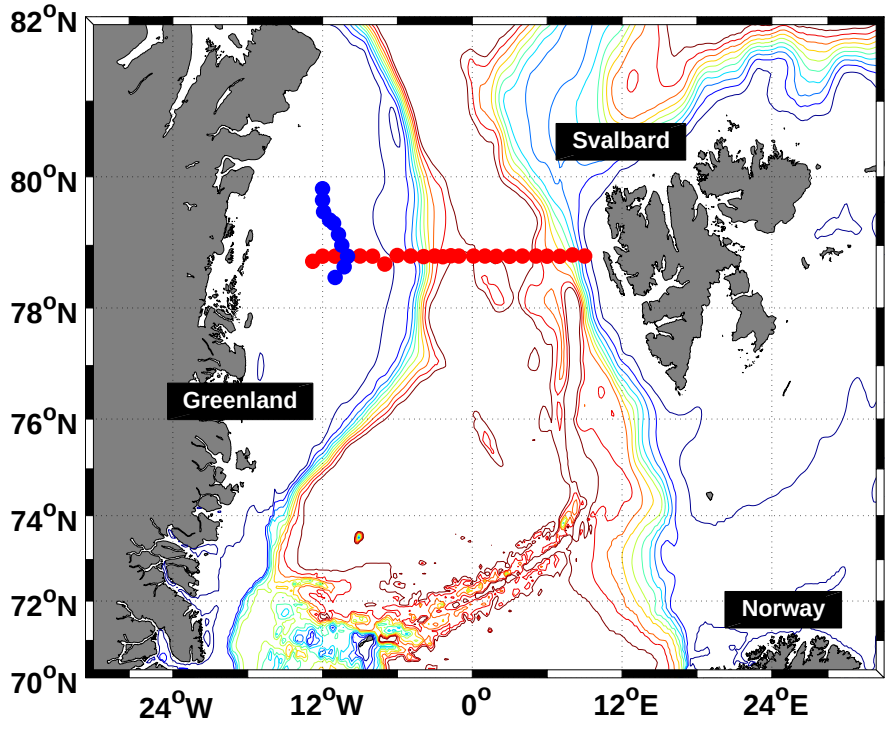

Fig. 1: Sample stations of the ARK-XXVII/1 cruise in 2012. The zonal stations are highlighted as red dots and the meridional stations along the fast ice edge as blue dots. The depth contours are 250:250:2500.

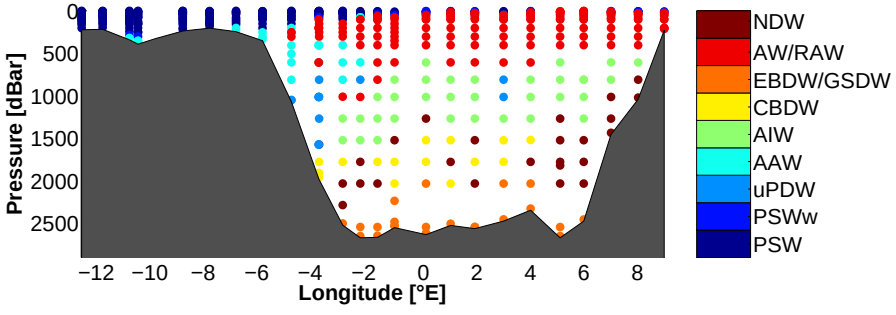

Fig. 2: Water masses in the Fram Strait: Nordic Seas Deep Water (NDW), Atlantic Water / Recirculating Atlantic Water (AW / RAW), Eurasian Basin Deep Water (EBDW) / Greenland Sea Deep Water (GSDW), Canadian Basin Deep Water (CBDW), Arctic Intermediate Water (AIW), Arctic Atlantic Water (AAW) / Return Atlantic Water (RAAW), Upper Polar Deep Water (uPDW), Polar Surface Water warm (PSWw) and Polar Surface Water (PSW).

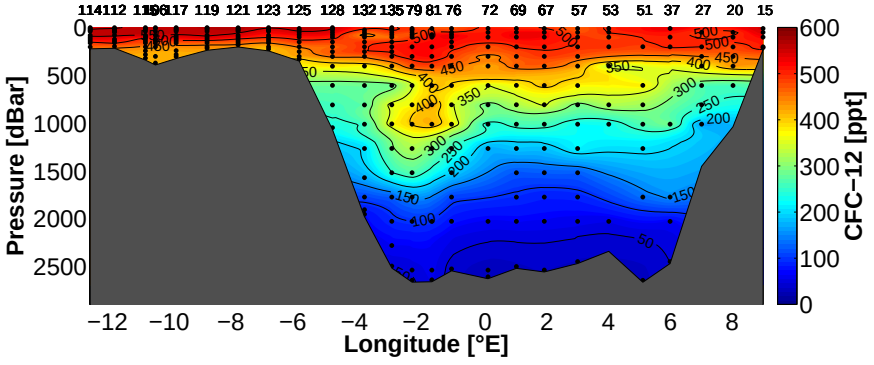

(a)

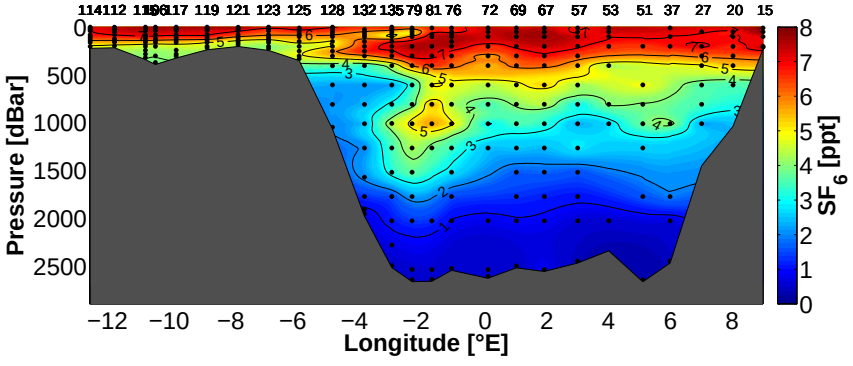

(b)

Fig. 3: Distribution of the partial pressure of(**a**) CFC-12 and (**b**) SF_6 along the zonal section in the Fram Strait.

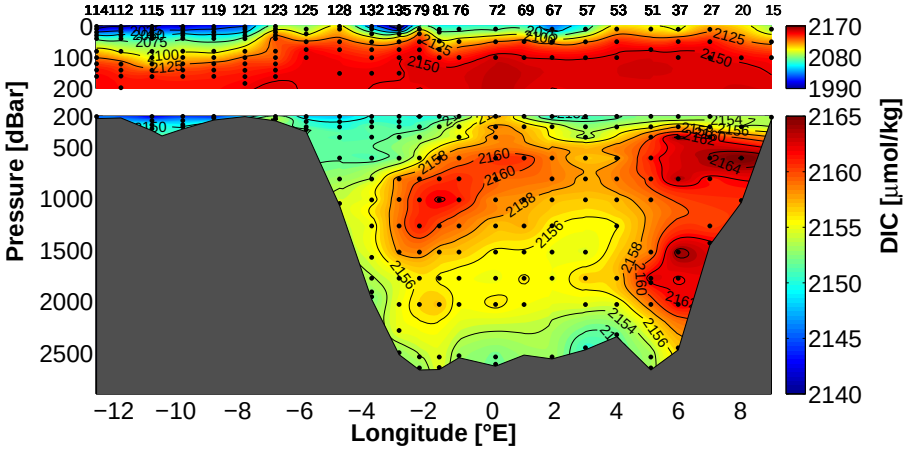

Fig. 4: Distribution of Dissolved inorganic carbon (DIC,in $\mu mol\, kg^{-1}$) along the zonal section in the Fram Strait.

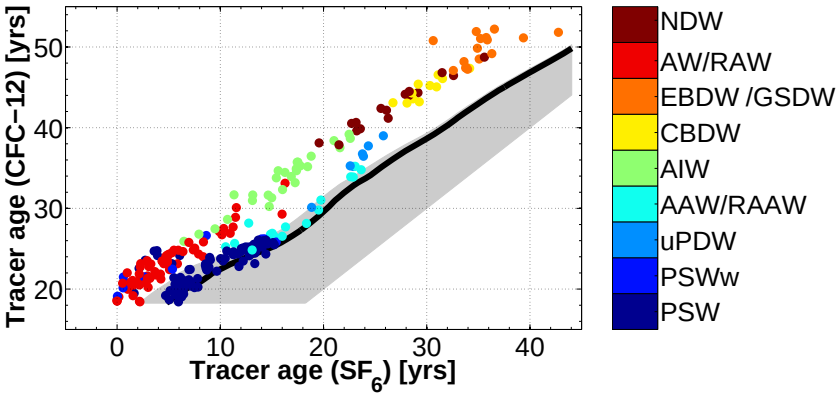

Fig. 5: Validity area of the IG-TTD defined by the tracer couple CFC-12 and SF_6 (grey shaded area). The black line indicates the IG-TTD based tracer age relationship using the unity ratio of $\Delta/\Gamma = 1.0$. The field data is colored by the type of water mass. The lower set (blue dots) describes surface and intermediate water of Arctic origin whereas the upper set includes water of Atlantic origin and deep water masses.

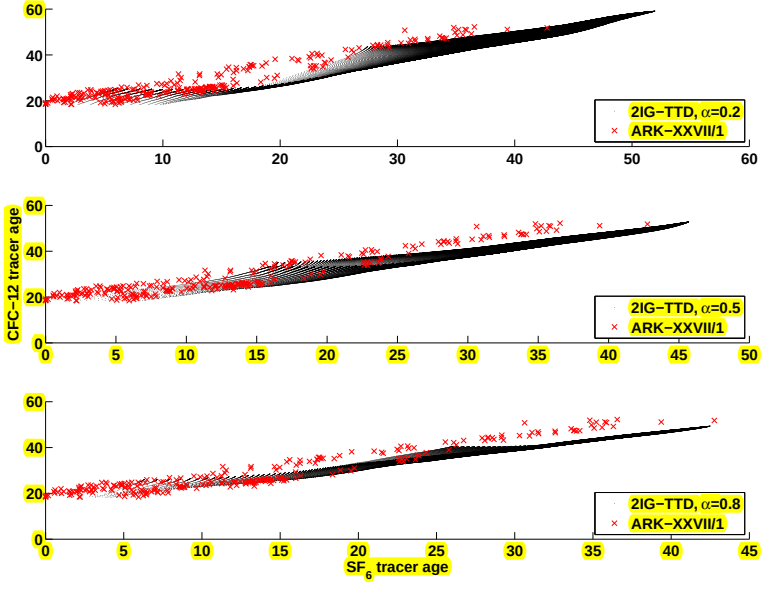

Fig. 6: Validity areas of linear combinations of two IG-TTDs for $\alpha = 0.2, 0.5, 0.8$, $\Delta_1/\Gamma_1 = 1.4$, $\Delta_2/\Gamma_2 = 0.6$ and $\Gamma_{1,2} = 1-500$ (black dots). The field data is described by the red crosses. The lower the α value the higher the share of the diffusively dominated IG-TTD.

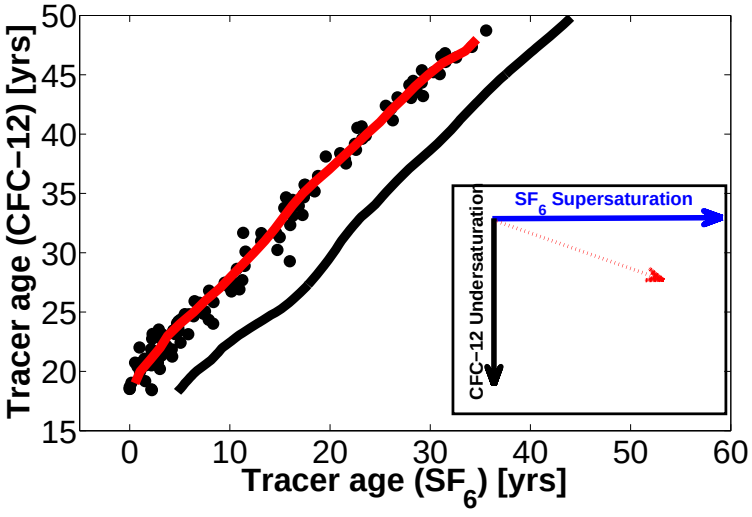

Fig. 7: Relation between the IG-TTD based tracer age relationship of the unity ratio (black line) and the mean tracer age relationship of the upper set of the field data (red line). The shape of both curves indicates similarities between the modelled and field data. The difference can be explained by undersaturation of CFC-12 and / or supersaturation of SF_6 (see inset).

Table 1: Mean ($\pm$ standard deviation) concentrations of anthropogenic carbon (C_{ant}) and mean age in the Fram Strait separated in water mass types.

Water mass	C_{ant} [$\mu mol\, kg^{-1}$]	**Mean age** [$years$]
AW/RAW	50 ($\pm$6)	9 ($\pm$10)
PSWw	46 ($\pm$5)	9 ($\pm$10)
PSW	43 ($\pm$2)	7 ($\pm$6)
AAW	38 ($\pm$5)	32 ($\pm$15)
AIW	31 ($\pm$5)	54 ($\pm$20)
uPDW	28 ($\pm$4)	69 ($\pm$19)
NDW	18 ($\pm$4)	143 ($\pm$44)
CBDW	15 ($\pm$2)	173 ($\pm$23)
EBDW/GSDW	11 ($\pm$1)	254 ($\pm$32)

Table 2: Flux estimates of DIC and anthropogenic carbon in the Fram Strait in 2012. Positive values describe poleward fluxes into the Arctic Ocean.

	Volume [Sv]	**Transport [Tg C yr^{-1}]**	
		DIC	**Anthropogenic carbon**
AW	4.4 ($\pm$3.2)	3592 ($\pm$2612)	78 ($\pm$57)
RAW/AAW	-3.5 ($\pm$1.9)	-2852 ($\pm$1549)	-67 ($\pm$36)
PW	-1.4 ($\pm$0.8)	-1118 ($\pm$639)	-23 ($\pm$13)
Σ	-0.5	-378	-12

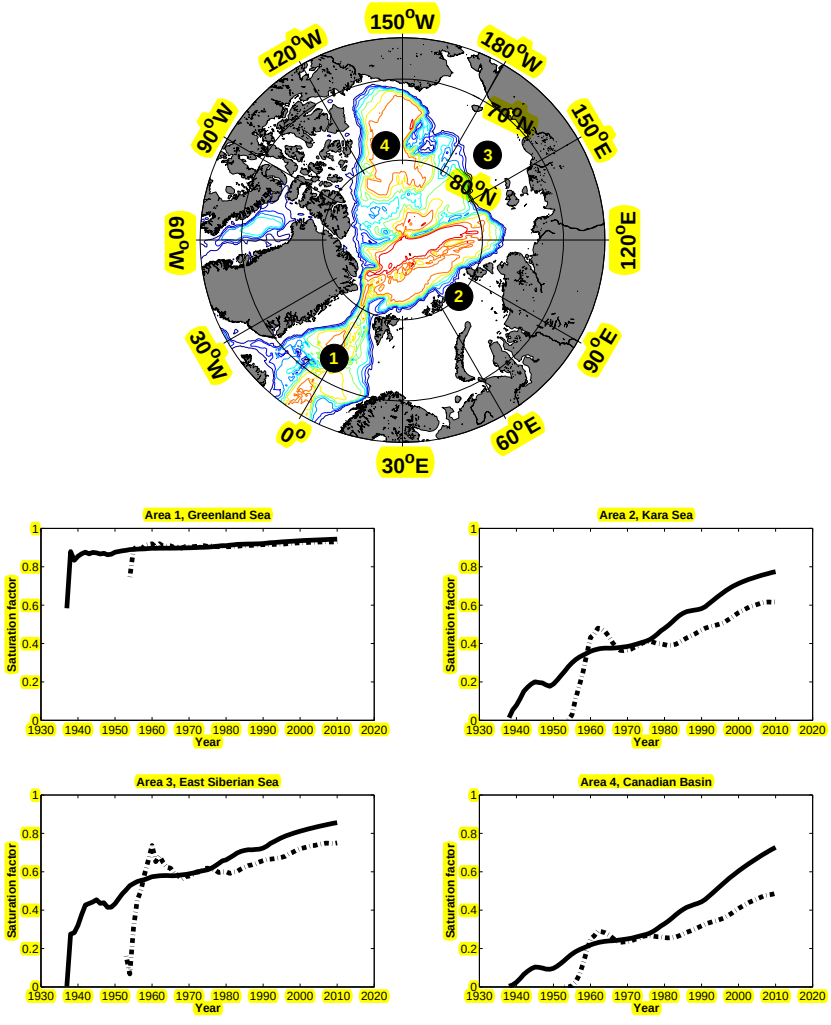

Fig. 8: Surface saturations of CFC-12 (black solid line) and SF_6 (black dash-dotted line) based on the model output of Shao et al. (2013). The model output shows mean values of the corresponding grids with a dimension of $300x300nm$ for typical source regions of different water mass types: (**1**) the Greenland Sea, (**2-3**) Arctic shelf regions and (**4**) Arctic open water / fast-ice region.

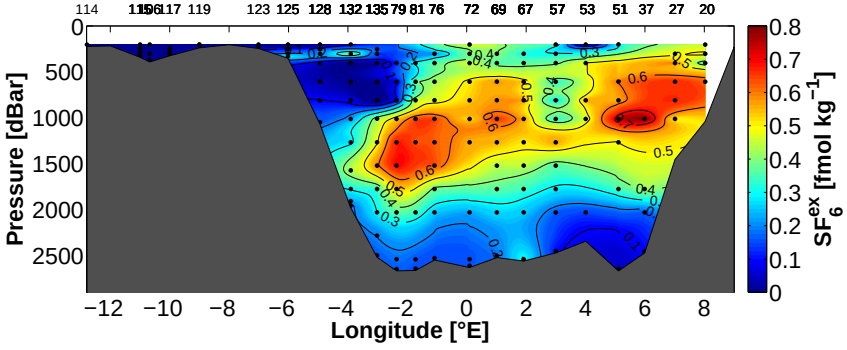

(a)

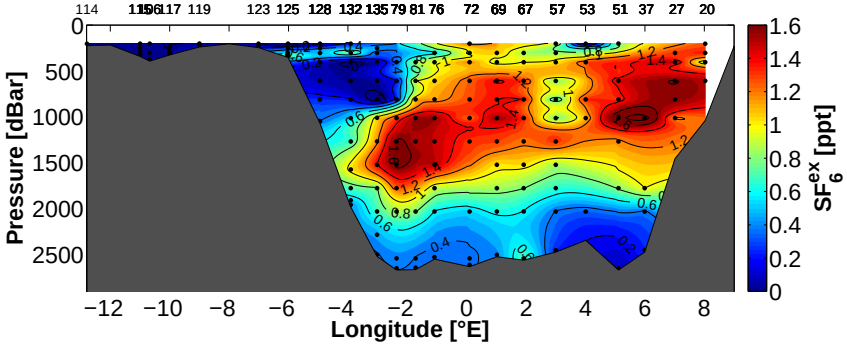

(b)

Fig. 9: Distribution of SF_6 excess (**a**) concentrations in $fmol\,kg^{-1}$ and (**b**) partial pressures in ppt. The upper $200\,m$ and station #15 cannot be calculated due to the atmospheric concentration limit of CFC-12 which inhibits an application of the IG-TTD.

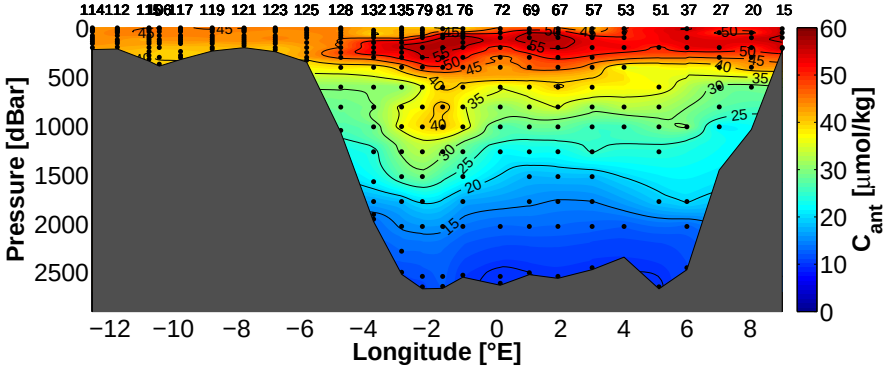

Fig. 10: Distribution of anthropogenic carbon in $\mu mol\,kg^{-1}$ along the zonal section in the Fram Strait.

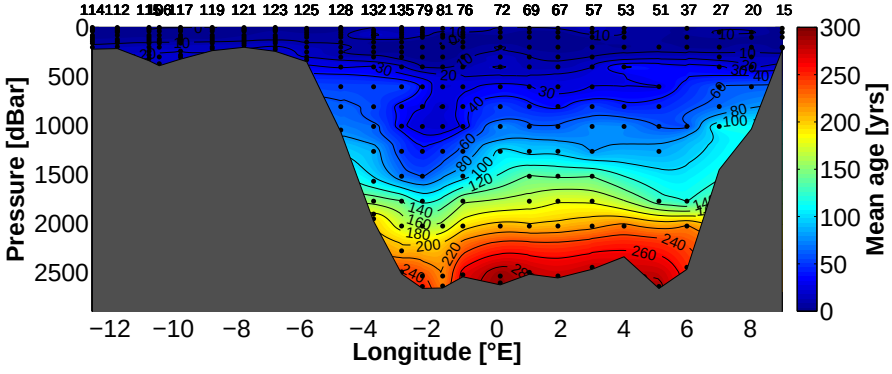

Fig. 11: Distribution of the mean age based on saturation corrected CFC-12 data below $100\,m$ and SF_6 data in shallower depths.

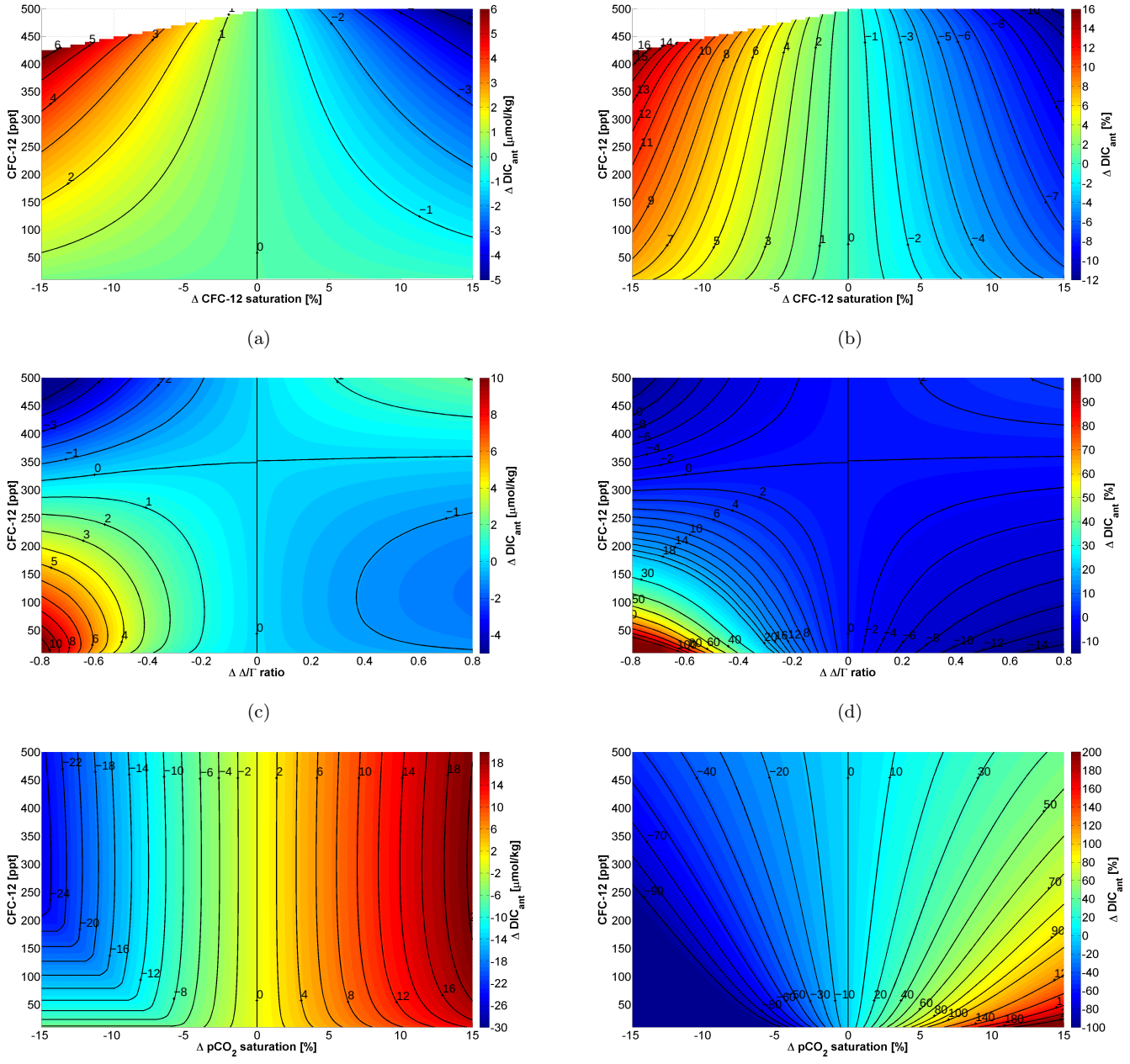

Fig. 12: Anthropogenic carbon concentration sensitivities as a function of CFC-12 concentrations vs. changes in (**a**, **b**) CFC-12 saturation, (**c**, **d**) Δ/Γ-ratio and (**e**, **f**) pCO_2 saturation. Deviations are stated in absolute (left panels) and relative (right panels) values. The reference points are defined by 100 % saturation of CFC-12 and pCO_2 and a ratio of $\Delta/\Gamma = 1.0$.